Agricultural and Forest Meteorology 315 (2022) 108815

Contents lists available at ScienceDirect

Agricultural and Forest Meteorology

journal homepage: www.elsevier.com/locate/agrformet

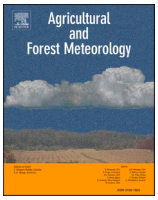

Modeling weather-driven long-distance dispersal of spruce budworm moths (*Choristoneura fumiferana*). Part 1: Model description

Matthew Garcia [a,*], Brian R. Sturtevant [b], Rémi Saint-Amant [c], Joseph J. Charney [d], Johanne Delisle [c], Yan Boulanger [c], Philip A. Townsend [a], Jacques Régnière [c]

[a] *Department of Forest and Wildlife Ecology, University of Wisconsin–Madison, Madison, WI 53706, USA*
[b] *USDA–Forest Service, Northern Research Station, Rhinelander, WI 54501, USA*
[c] *Natural Resources Canada, Canadian Forest Service, Quebec G1V 4C7, Canada*
[d] *USDA–Forest Service, Northern Research Station, Lansing, MI 48910, USA*

ARTICLE INFO

Keywords:
Aerobiology
Individual-based modeling
Insect outbreaks
Lepidoptera
Numerical modeling
Weather radar

ABSTRACT

Long-term studies of insect populations in the North American boreal forest have shown the vital importance of long-distance dispersal to the maintenance and expansion of insect outbreaks. In this work, we extend several concepts established previously in an empirically-based dispersal flight model with recent work on the physiology and behavior of the adult eastern spruce budworm (SBW) moth, *Choristoneura fumiferana* (Clemens). An outbreak of defoliating SBW in Quebec, ongoing since the mid-2000s, already covers millions of hectares of forests in eastern Canada and threatens to spread into neighboring areas through annual summertime episodes of long-distance dispersal. Such flight events in favorable conditions frequently include billions of SBW moths dispersing in the warm atmospheric boundary layer, typically starting around sunset and often lasting through several hours of wind-driven transport over hundreds of kilometers. Successful SBW dispersal to possibly distant host forest areas depends acutely on the weather. Here we describe the components and results of SBW–pyATM, an open-source individual-based modeling framework developed in Python for the simulation of these weather-driven SBW dispersal events. Using seasonal SBW phenology results from BioSIM at known outbreak locations and high-resolution Weather Research and Forecasting (WRF) model output, we focus on modeling dispersal flights over two successive nights in July 2013 in southern Quebec. Our flight model closely reproduces the SBW spatial patterns and motions observed by weather surveillance radar over the St. Lawrence estuary. With SBW–pyATM we can estimate landing locations for both male and female SBW and the resulting spatial patterns of egg distribution, allowing us eventually to forecast future larval defoliation activity in new locations where immigration could help overcome local limitations on SBW populations. This information could then support forest management decisions where SBW outbreaks threaten valuable resources.

1. Introduction

Outbreaks of defoliating insects significantly affect forest health, but the processes underlying their occurrence, growth and regional synchrony are complex, and spatiotemporal prediction of outbreak behavior is therefore difficult. Four primary processes govern outbreak growth and synchronization over large regions: (1) Allee effects (Stephens et al., 1999; Taylor and Hastings, 2005; Régnière et al., 2013, 2019a); (2) neighborhood effects of natural enemies (Berryman, 1982, 1996; Parry et al., 1997; Bouchard et al., 2018a); (3) density-driven dispersal (Smith et al., 2008; Lakovic et al., 2015; Bonte and Dahirel, 2017; Régnière and Nealis, 2019), including long-distance dispersal and migration in some taxa (Chapman et al., 2015); (4) Moran effects (Peltonen et al., 2002; Liebhold et al., 2004) due to exogenous factors, such as weather favoring outbreak phenology over large areas. It is often challenging to disentangle these processes in observational studies: these processes are inherently difficult to quantify on their own and depend to some degree on each other's outcomes. Allee effects, Moran effects, and local (neighborhood) effects such as predation have received much attention over the past several decades, but even the most complex models developed to investigate insect outbreaks at various spatiotemporal scales have yet to include all these factors as distinct processes.

* Corresponding author.
E-mail address: matt.e.garcia@gmail.com (M. Garcia).

https://doi.org/10.1016/j.agrformet.2022.108815
Received 27 September 2021; Received in revised form 3 January 2022; Accepted 5 January 2022
Available online 13 January 2022

There is a growing recognition of dispersal and migration as an important phase in the life history of various insects (Chapman et al., 2015; Bonte and Dahirel, 2017; Satterfield et al., 2020) and increasing interest in long-distance dispersal (perhaps 10 km or more) as a discrete component of insect outbreak behavioral models. Recent studies of long-distance moth dispersal have generally focused on agricultural pests such as corn cutworms (Showers et al., 1989; Showers, 1997), corn earworms (Westbrook et al., 2014; Wu et al., 2018), armyworms (Westbrook et al., 2016, 2019; Westbrook and Eyster, 2017), sugarcane aphids (Wang et al., 2019, 2021; Koralewski et al., 2021), and numerous additional taxa. Whereas these and most previous studies have focused on agricultural pest dispersal in temperate and tropical climates, here we model the dispersal of a forest defoliator that is endemic to the boreal region of North America.

We focus in this work on observations and modeling of wind-driven dispersal for the adult spruce budworm (SBW), *Choristoneura fumiferana* (Clemens) (Lepidoptera: Tortricidae), in eastern Canada. The larval SBW feeds on the needles of boreal evergreen tree species (Hennigar et al., 2008) including balsam fir (*Abies balsamea* L., Mill.), white spruce (*Picea glauca* Moench, Voss), red spruce (*P. rubens* Sargent), and black spruce (*P. mariana* Mill., Briton, Sterns & Poggenburg). Outbreak densities of SBW in eastern Canada typically recur on a 35- to 40-year cycle and last 5–25 years, with a mean outbreak duration of 10.2 y and standard deviation of 3.8 y (Boulanger and Arsenault, 2004; Boulanger et al., 2012). The present outbreak in southern Quebec started *ca.* 2003 (Bouchard and Auger, 2014) and at the time of this publication covers more than 13 M ha in Quebec and surrounding areas. The previous outbreak in Quebec, spanning approximately 1976–1991, also lasted longer than the historical mean outbreak duration in this region and eventually affected ~55 M ha of boreal forest species in Canada and adjacent portions of the United States. Repeated annual defoliation of host trees at outbreak severity can lead to widespread forest mortality (MacLean, 1980) and altered forest succession (Bouchard et al., 2007).

The temperature-dependent process of SBW larval development on host trees has been covered in detail by previous work (Régnière et al., 1995; Régnière, 1996, 2014) and codified in the BioSIM modeling framework (Régnière et al., 2012). Dispersal of adult SBW moths occurs during the reproductive period following pupation and has been observed and described empirically by several researchers (Greenbank et al., 1980; Dickison et al., 1983, 1986, 1990; Pedgley et al., 1990). Over the entire area covered by the current SBW outbreak in eastern Canada, the adult dispersal period typically spans 6–8 weeks of the summer (Régnière et al., 2012) with local peaks in flight activity depending on local phenology and weather during July and August. The effects of weather on SBW flights are among the most thoroughly studied across numerous insect taxa. Greenbank (1957) and Greenbank et al. (1980) advanced the field of aerobiology with radar, aerial, and direct observations linking SBW dispersal events on individual nights to the immediate weather conditions. In observations during the 1980s SBW outbreak in New Brunswick, Dickison et al. (1983, 1986) and several others recorded and analyzed the response of SBW to storm events during dispersal flights. Riley et al. (1983) proposed that long-distance dispersal may be followed by re-concentration in new locations of favorable habitat. In subsequent analyses, Dickison et al. (1990) and Pedgley et al. (1990) identified both large-scale weather features and local near-surface convergence zones that helped to concentrate dispersing SBW near the end of their flights.

Some studies of SBW, *e.g.*, Royama (1984, 2005), have dismissed dispersal and migration as a major cause of outbreak spread and population cycle synchronization, arguing instead that Moran effects and density-dependent local processes govern the regional synchronization of insect outbreaks. Other research, including studies focused on the increasing phase of SBW outbreaks, challenge that paradigm. SBW emigration, the departure of adults from a given location, is best understood as a density-dependent process resulting from crowding and deteriorating habitat conditions (including ongoing defoliation), both of which can affect the expected availability of food resources for the next generation of SBW during the outbreak (Régnière and Nealis, 2007; 2019; Van Hezewijk et al., 2018; Rhainds, 2020). Dispersal of adult SBW is also thought to support the redistribution and mixing of subpopulations and to promote both spatial synchrony in SBW outbreaks over large areas (Régnière and Lysyk, 1995; Williams and Liebhold, 2000; Peltonen et al., 2002; Nenzén et al., 2018; Régnière and Nealis, 2019) and the endemic persistence of SBW populations between outbreak events (Bouchard and Auger, 2014; Bouchard et al., 2018b). Theoretically, several years of flight-supporting weather can help local populations overcome Allee effects (Nealis and Régnière, 2004; Régnière et al., 2019a), including potential mating failure (Contarini et al., 2009; Tobin et al., 2009; Rhainds, 2010; Régnière et al., 2013). Repeated immigration, the arrival of both male and female SBW to favorable host forest locations, can even thwart human efforts to halt incipient outbreaks, as recently demonstrated by the SBW Early Intervention Strategy in New Brunswick (Johns et al., 2019; MacLean, 2019; MacLean et al., 2019; Régnière et al., 2019b).

We have developed a computational framework for modeling SBW dispersal flight events that we have dubbed the Python-based Atmospheric Transport Model for Spruce Budworm (SBW–pyATM). This model is based primarily on the work of Sturtevant et al. (2013), who developed an individual-based flight model for SBW dispersal in the region of the Upper Great Lakes using several behavioral parameterizations from the work of Greenbank et al. (1980) and a three-phase paradigm for insect flight proposed by Scott and Achtemeier (1987) and Isard et al. (2005). We have updated several components of the flight model using recent work on SBW physiology and temperature-dependent behavior by Régnière et al. (2019c, 2019d), relaxing several assumptions applied in Sturtevant et al. (2013) regarding liftoff timing and flight altitude. In the SBW–pyATM framework, the dates of adult SBW emergence from pupation (and thus their availability for mating and flight) are obtained from BioSIM (Régnière et al., 2012). The dispersing SBW "agents" in our individual-based model then behave in direct response to high-resolution meteorological conditions obtained using the Weather Research and Forecasting (WRF) model (Skamarock and Klemp, 2008; Skamarock et al., 2008; Powers, 2017).

Weather surveillance radar can provide valuable information on insect spatial distributions and their volume-averaged speed and direction during a flight. Boulanger et al. (2017) related processed operational Doppler weather radar observations over the current SBW outbreak region in southern Quebec to moth dispersal behavior and the flight environment. Early radar-based studies of SBW dispersal in eastern Canada generally focused on the overall speed and direction of large masses of flying moths in combination with field-based visual observations (Greenbank et al., 1980) and aircraft collections under clear-sky conditions (Greenbank et al., 1980; Dickison et al., 1986). Detailed radar observations of moth flights (Drake, 1984, 1985; Reynolds et al., 2005, 2008; Wood et al., 2006, 2009, 2010; Chapman et al., 2016) have provided valuable insights into the effects of atmospheric conditions on insect dispersal and migration, including observations of vertical layering and wind-relative flight orientation of several different taxa. These findings suggest several potentially common flight behaviors, especially an acute sensitivity across species of moth flight to the vertical temperature profile in the atmospheric boundary layer. Several recent studies have shown that Doppler radar (Westbrook et al., 2014; Boulanger et al., 2017; Westbrook and Eyster, 2017) and polarimetric weather radar (Zrnic and Ryzhkov, 1998; Westbrook and Isard, 1999; Stepanian et al., 2016; Gauthreaux and Diehl, 2020) can provide spatiotemporally detailed information that can help improve physical descriptions of individual insect flight behavior.

In this paper we describe the flight model components and the overall SBW–pyATM model framework. We further demonstrate several simulation results focused on an area of southern Quebec where SBW dispersal events occurred and were observed by operational weather

radar over two nights, from 14 to 16 July 2013 (Boulanger et al., 2017). In Part 2 of this series, we will show how we have used that radar data to calibrate several parameters of this model that do not yet have empirical derivations to reduce model uncertainty and to quantitatively validate specific flight model results. In future work, we will compare calibrated flight model predictions with several ground-based observations of SBW activity during the 2013 summer dispersal period in southern Quebec.

2. Study area

Large forest areas in eastern Canada and growing areas in the northeastern United States are affected by an ongoing SBW outbreak that started in southern Quebec *ca.* 2003 (Bouchard and Auger, 2014) and by 2013 covered ~3.2 M ha in that region (Fig. 1). Host tree species for the SBW are integrated into a predominantly mixed (deciduous and coniferous) boreal and sub-boreal forest landcover matrix covering much of the region (Fig. S1). The foci of the present outbreak in Quebec, primarily in locations associated with river valleys (Fig. S2), were identified by aerial surveys (MacLean and MacKinnon, 1996; Candau et al., 1998; Taylor and MacLean, 2008) and have persisted in the St. Jean Lake, North Shore, and Lower St. Lawrence regions (Fig. 1).

The Environment Canada weather surveillance (Doppler) radar located in Val-d'Irène, Quebec (XAM; 48.4783ºN, 67.5822ºW, 722 m above mean sea level; location marked in Fig. 1), recorded cross-estuary SBW flights on several evenings in July 2013 during a period of peak dispersal activity (Boulanger et al., 2017). In this paper we examine dispersal during the nights of 14–15 and 15–16 July 2013 because of the large numbers of SBW moths that passed through the XAM coverage area in different directions and under different weather conditions. These radar data proved valuable for the comparison of SBW dispersal model results with nightly flight observations in this work.

3. Methods

To structure this description of the individual-based SBW–pyATM framework, we have adopted the ODD protocol ("Overview," "Design," and "Details"; Grimm et al., 2006, 2010). This protocol standardizes and streamlines the description of modeling activities where the description of individual simulation agents is required. We have supplemented the ODD descriptive structure with a section regarding computational methods and resources, an important consideration when defining the geographic area, model capabilities, and extent of exploration and experimentation achievable for an individual- or agent-based simulation activity.

3.1. Overview

The Python-based Atmospheric Transport Model for Spruce Budworm (SBW–pyATM) is an individual-based model for the simulation of SBW adult moth dispersal events in summer. Moth availability following summer eclosion (emergence from pupation) and mating is provided by the BioSIM modeling framework. Weather conditions based on WRF simulations are provided to the simulation at a high spatiotemporal resolution so that storm conditions, nocturnal transitions, and terrain effects on low-level winds are accounted for. The liftoff, flight, and landing behavior of individual SBW moths are determined in response to weather conditions, especially temperature and wind, to calculate the dispersal of SBW over a given night. The SBW–pyATM framework allows for ensemble simulations to represent large dispersal events and accounts for the sex of dispersing moths. The model tracks both female SBW fecundity, providing an estimate of egg quantities deposited in liftoff and likely landing locations, and the movement (and thus mating availability) of male SBW, to inform about potential future outbreak locations.

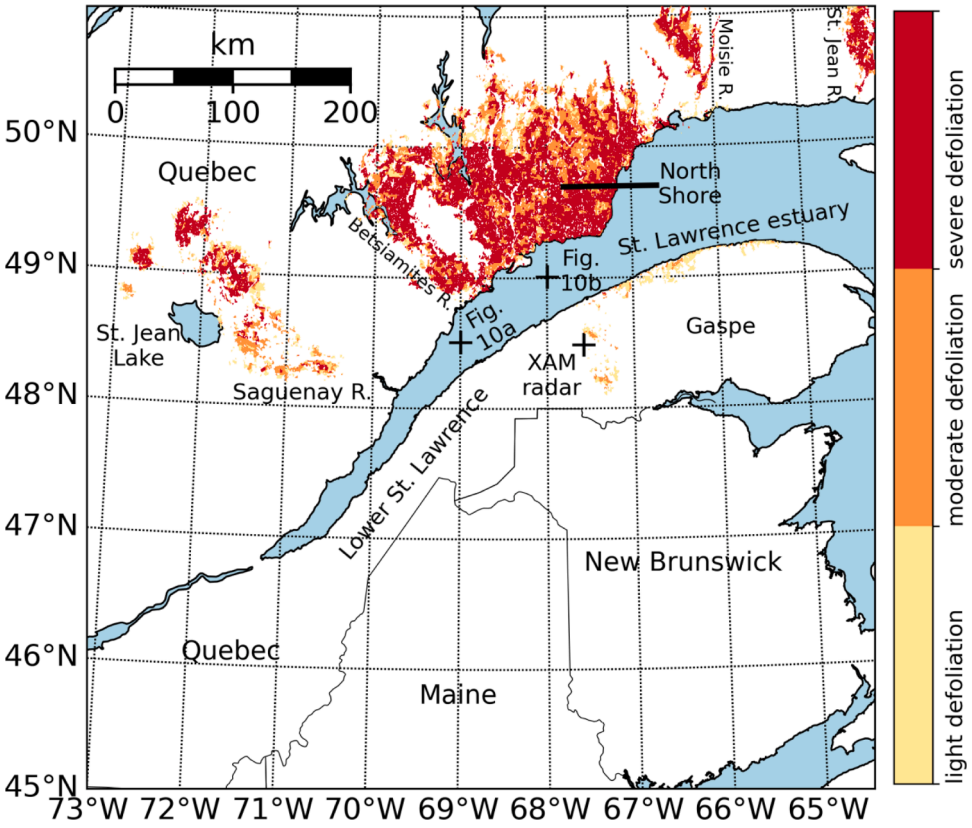

Fig. 1. Defoliation severity in SBW host forests in eastern Canada and the northeastern United States, based on aerial surveys in summer 2013. The extent of host forests in this region is shown in Fig. S1.

3.2. Design

Our individual-based model of SBW dispersal is supported by two loosely coupled models, from which simulation results are used as input to the pyATM simulations. The organization of the flow of information through this collection of models is illustrated in Fig. 2. Several external information sources, such as topography and land cover categorization, are used by multiple modeling components. The BioSIM modeling system (described further below) draws its own meteorological information from available resources to calculate the growth and development of SBW, providing the estimated dates of adult emergence across the study area. At that time, the physiological characteristics of the adult SBW (sex, mass, wing area) are determined by random selection from known distributions (Régnière et al., 2019c). Both the emergence dates and characteristics of thousands of moths tracked by BioSIM are then provided to the SBW–pyATM input processing procedures. With the WRF model (also described further below) we generate hourly output in three spatial dimensions covering the study area over an entire night of anticipated SBW dispersal, which we then provide to the SBW–pyATM simulation procedure for the calculation of insect behavior before liftoff, during the dispersal flight, and during landing.

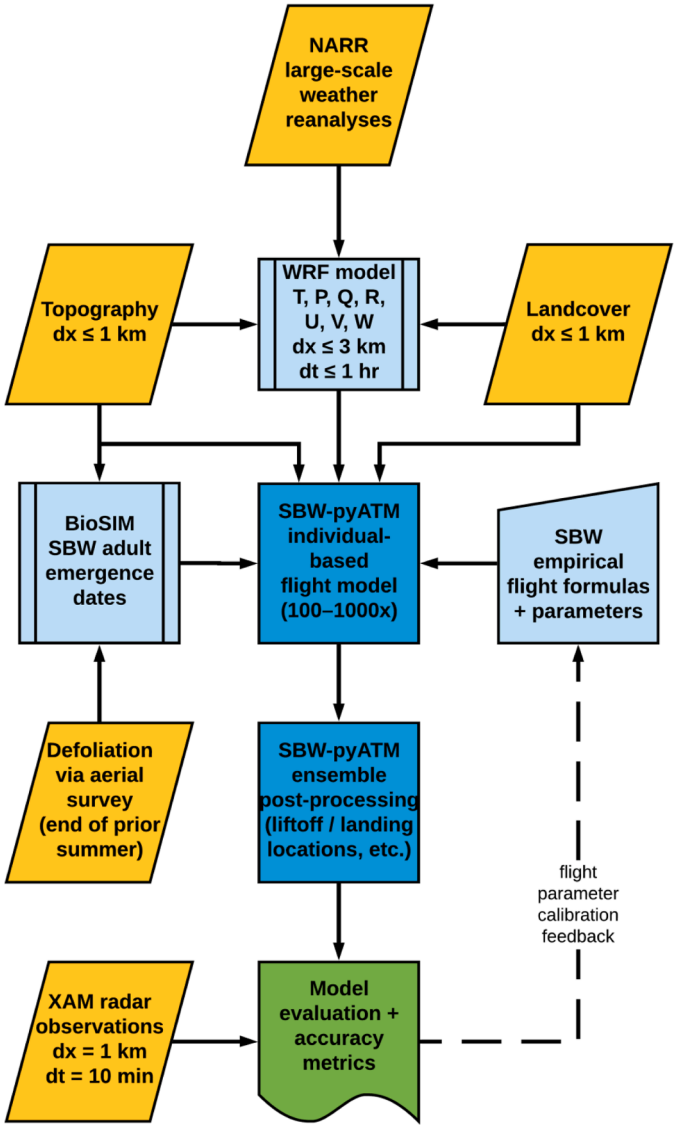

Fig. 2. Conceptual diagram of the SBW–pyATM framework, including modeling procedure and data processing stream.

We have developed and programmed the SBW–pyATM on an object basis: each moth is treated as an individual that carries information regarding its own unique identification, sex, morphology (including fecundity/gravidity for females), location, environment, and flight activity throughout the simulation. All moths in the simulation are subjected to a common set of behavioral rules regarding the effects of their environment in the forest canopy, at liftoff, and during dispersal flight and landing. A complete picture of each moth's physical state, location, and environment can be reconstructed from its flight simulation record to illustrate various controls exerted by temperature, topography, and wind patterns through the night. At the end of each simulation replicate, and when all replicates in a simulation ensemble are completed, we use several post-processing routines to summarize and illustrate the modeled flight trajectories, liftoff and landing locations, egg deposition, and export/import of fecundity. The design of the present model structure (Fig. 2) will allow for expansion to include additional ecosystem processes such as the SBW mating process and more detailed egg deposition calculations while requiring minimal changes to the existing components. This flexibility and extensibility of our SBW modeling system will facilitate numerous additions and upgrades to include components that will be vital to a full-season simulation of SBW dispersal dynamics.

3.3. Details

3.3.1. Ancillary modeling: BioSIM

Information regarding the availability (date of eclosion) and morphology (sex, mass, and wing size) of individual SBW adult moths within the simulation region is provided by the BioSIM modeling framework. BioSIM provides daily temperature input for insect seasonal biology models (Régnière et al., 1995; Régnière, 1996; Régnière et al., 2014). BioSIM collects available weather station data and accounts for station proximity, topography, and local thermal gradients to generate daily maps of minimum and maximum temperatures (Régnière and Bolstad, 1994; Régnière, 1996; Régnière and Saint-Amant, 2007). These temperature fields are then used to drive an individual-based SBW seasonal biology model (Régnière et al., 2012). BioSIM was applied only within the known defoliated area based on aerial survey observations (Fig. 1). Model output provides moth location, date of adult SBW eclosion in summer 2013, and individual body morphology including sex, forewing area, mass, and female fecundity for each moth in the simulation. Using those output data, we then calculated the median date of SBW eclosion at each BioSIM modeled location for the 2013 summer (Fig. S3).

To provide a large and varied population of SBW moths to our flight simulations, for each night of dispersal simulation we take the entire list of BioSIM SBW moths that had emerged on or before one day prior to the flight simulation date, giving all of them this marginal "emergence" date. Because newly mated SBW females are thought to fly only short distances, if at all (Sanders and Lucuik, 1975; Sanders et al., 1978; Régnière, 1983; Rhainds and Kettela, 2013), we allow this one-day gap so that, theoretically, emergent females would then mate and undergo one round of oviposition at their natal location. By the second night after emergence, we can explicitly assume that all these moths are available and ready for flight. For each simulation using the SBW–pyATM model, we then select a random subset of the available SBW moths (typically ~1000 moths per simulation replicate) without regard for their location in the defoliated area. We found in test simulations that this procedure for random selection often led to a geographic bias in each flight simulation replicate, with more moths arising from the areas where adults had been emerging for a longer portion of the summer. We have attempted to mitigate that bias primarily with numerous simulation replicates for this work.

Implicit (at present) in these procedures linking BioSIM results to SBW–pyATM flight simulations is an assumption of independence and non-interaction between dispersal simulation nights, even two nights in

succession as we show here. In this version of SBW–pyATM, we apply the same procedure for the selection of available moths for the second night as we applied for the first night, with two major implications. First, in considering the moths available for flight on the second night, we do not remove those that may have (or were shown in our simulations to have) dispersed on the first night. Second, though moths surviving their first dispersal flight should then be capable of additional dispersal flights on subsequent nights, we do not consider here those SBW moths that disperse on the first night of simulations as available, in their new locations, for dispersal on the next night. Procedures to address these uses of the BioSIM-provided data are part of ongoing improvements to the SBW–pyATM modeling procedure, especially its extension to dispersal over multiple nights, which will be demonstrated in future work.

3.3.2. Ancillary modeling: WRF

Complete weather information (temperature, winds, and precipitation) within the study region for simulated dispersal flight dates, necessary for the determination of individual flight behavior, is provided by the Advanced Research WRF model (v4.01; Skamarock and Klemp, 2008; Skamarock et al., 2008; Powers, 2017). WRF is a widely used three-dimensional, non-hydrostatic, mesoscale atmospheric model. Additional details regarding our WRF model configuration are given in the Supplemental Materials, including our grid layout (Fig. S4, Table S1) and parameterization selections (Table S2). We apply WRF to the dynamically consistent reduction of large-scale NOAA–NCEP North American Regional Reanalysis (NARR: Mesinger et al., 2006; Luo et al., 2007) meteorological data products from their native spatiotemporal resolution ($\Delta x = \sim 32$ km and $\Delta t = 3$ h) to a higher spatiotemporal resolution ($\Delta x = 3$ km and $\Delta t = 1$ h) in the region of interest. We then process the WRF output files for the rotation of grid-based wind vectors to eastward–northward (x–y) components and to extract the specific surface and upper-air weather fields (up to an altitude of 2 km above mean sea level) for use in the dispersal flight model.

3.3.3. Individual-based modeling: SBW–pyATM

Our model for weather-driven insect dispersal follows directly on the work of Sturtevant et al. (2013), who used observations by Greenbank et al. (1980) of SBW flight conditions and behavior to parameterize an individual-based flight model. That model brought together several of the elements necessary for SBW dispersal modeling: accurate surveys of outbreak locations and host forests, high-resolution weather conditions derived from WRF, and a rule-based flight model that made several simplifying behavioral assumptions with a strong reliance on the work by Greenbank et al. (1980).

Recent research efforts have refined our understanding of physiological controls on SBW flight, especially several behaviors that were addressed qualitatively by Greenbank et al. (1980) including functional relationships between the time of day, temperature, and the ability of SBW to lift off for flight above the forest canopy. Specifically, Régnière et al. (2019c) examined temperature constraints on SBW physiological flight capabilities, and Régnière et al. (2019d) extended temperature-dependent limitations on liftoff to describe the circadian (evening crepuscular) rhythm of observed SBW dispersal activity. Our SBW–pyATM framework and dispersal flight model retain the individual-based conceptual framework for insect atmospheric transport developed by Sturtevant et al. (2013), including division of the flight process into three successive phases (liftoff, dispersal flight, and landing) based on the work of Scott and Achtemeier (1987) and Isard et al. (2005), and incorporates the recent improvements to the description of SBW flight timing and physiological behavior by Régnière et al. (2019c, d) (see Table S3) in a modular, object-based, Python (v3.8+) open-source numerical application. The local temperature and wind speed vary throughout a moth's flight, interacting with the SBW moth's individual morphological characteristics (wing area, body mass, and wingbeat frequency) to affect all flight stages from ascent speed at liftoff, to flight altitude and horizontal flight speed during dispersal, and to landing behaviors that may be affected by additional external factors (*e.g.*, sunrise and precipitation). In operation, SBW–pyATM calculates and updates the activity and locations of individual moths on a user-specified time step (default $\Delta t = 60$ s) over the evening and night according to weather conditions provided in the WRF-derived fields.

Liftoff phase: Greenbank et al. (1980) described the liftoff phase of the SBW as the decision to launch from the forest canopy, followed by active flight upward and into the wind, before transitioning to downwind flight well above the canopy. The liftoff phase in the SBW–pyATM corresponds with this observed sequence of flight behavior. Liftoff timing for a given moth is determined by the observed circadian rhythm of SBW dispersal flight behavior (Régnière et al., 2019d) using a Gaussian temporal distribution of liftoff likelihood that is shifted relative to local sunset by a temperature-dependent function. In practice, each moth is also assigned a random value from a uniform distribution at the beginning of the simulation, when its time- and temperature-dependent liftoff likelihood function is calculated. Once the value of the moth's time-dependent liftoff likelihood function exceeds its assigned random value, liftoff can occur at any time that the moth's temperature-dependent wingbeat frequency exceeds that required to hold the moth's mass aloft (Régnière et al., 2019c), a condition that typically diminishes through the evening.

The SBW liftoff conditions include two additional constraints. The first is a threshold maximum precipitation rate ($R_{max} = 2.5$ mm/h) carried over from Sturtevant et al. (2013). We note, however, that precipitation constraints on moth liftoff were not applicable on the dates we examine in this paper. The second liftoff constraint accounts for an observation by Greenbank et al. (1980) that SBW moths do not fly in calm wind conditions, though the "calm" threshold was not precisely defined. Here we define this calm wind condition as some minimum horizontal wind speed $V_{h,\min}$ below which a moth will not lift off:

$$V_h = \sqrt{U^2 + V^2} < V_{h,min}, \tag{1}$$

where V_h is the horizontal wind speed and U and V are the eastward (x) and northward (y) horizontal wind components, respectively. The parameter $V_{h,\min}$ has not been determined empirically from field observations, but we conclude through simulation-based analysis that its value is likely near $V_{h,\min} = 1.5$ m/s. That analysis will be presented in Part 2 of this work.

Greenbank et al. (1980) also observed that SBW moths sometimes lift off with adequate surface winds only to find calm conditions aloft, leading the moths to settle back into the forest canopy. Our model reproduces this behavior by allowing a moth that lifts off to climb at its temperature-determined velocity v_z (see below) to a "decision level" at ~60 m above ground level (AGL), well above the forest canopy (typically ~15–25 m AGL) to account for turbulence due to canopy roughness. When the moth reaches that level we apply the "calm wind" test again and, if $V_h > V_{h,\min}$ is still true, the moth transitions to the downwind dispersal phase of flight. If not, the moth drops back into the forest canopy where it is allowed to lift off again within the same night if suitable conditions re-occur. Moths are allowed to lift off three times over the course of a single night, a limitation that we have imposed as a proxy for possible exhaustion of the moth's energy reserves due to multiple liftoff attempts.

Dispersal phase: The dispersal phase of flight is the period from the initiation of downwind flight following liftoff (upon passing the decision level) until either the initiation of the landing phase or the direct intersection of a moth's trajectory with the forest canopy, ground, or water surface. A moth's flight velocity (v) is modified by the wind in both the vertical (z) and horizontal (h, in the x–y plane) directions, and the moth's horizontal flight direction is always the same as the horizontal wind vector:

$$v_{z,g} = W + v_z, \tag{2}$$

and

$$v_{h,g} = V_h + v_h = \sqrt{U^2 + V^2} + v_h, \quad (3)$$

where the subscript "*g*" indicates the ground-relative velocity and [*U, V, W*] are the local wind components in the east–west (*x*), north–south (*y*), and vertical (*z*) directions, respectively, as provided by the WRF model output. The moth's wind-relative flight velocity in the horizontal direction v_h, and its ascent or descent v_z relative to the vertical wind, are functions of individual moth morphology (*i.e.*, mass and wing area) and the temperature-dependent wingbeat frequency (Régnière et al., 2019c).

The formulation for wind-relative vertical motion proposed by Régnière et al. (2019c) was:

$$v_z = \alpha\,[\nu(T) - \nu_s], \quad (4)$$

where the term in brackets represents "excess wingbeat frequency" beyond that required to keep the moth in settled (level) flight (ν_s, which depends strictly on *A* and *M*) at the environmental temperature *T* and ignoring any vertical wind component. The value $\alpha = 0.11$ m s^{-1} Hz^{-1} assumed by Régnière et al. (2019c) was selected to yield a range of vertical velocities "commensurate with observed ascent rates," referring to visual estimates of liftoff vertical velocity provided in Greenbank et al. (1980). Let us consider this excess wingbeat frequency formulation with no such differential, such that $v_z = 0$ indicating level flight (in the absence of any vertical environmental wind). This is the situation suggested by purely horizontal SBW dispersal flight, as imposed by Sturtevant et al. (2013) at an altitude based on radar observations by Schaefer (1976) in a stable atmospheric boundary layer. However, in this model, we allow an additional (vertical) degree of freedom based on Régnière et al. (2019c). As the moth enters warmer air, its wingbeat $\nu(T)$ becomes greater than ν_s leading to $v_z > 0$, such that the moth ascends until it reaches the altitude of its new thermotaxic equilibrium. Likewise, entering cooler air diminishes that wingbeat $\nu(T)$ leading to $v_z < 0$ and descent toward warmer air until a new thermotaxic equilibrium is achieved or landing occurs. In a boundary layer where temperature decreases with height, as in the few hours after sunset on many nights, this formulation is stable: the moth climbs through increasingly cooler air until it reaches a level at which the temperature limits further ascent. More complex situations, especially those involving atmospheric inversion layers (in which the temperature increases with altitude) can complicate the expected patterns of moth flight through simple physiological response to its environment.

Régnière et al. (2019c) also showed measurements of SBW moth mass and wing area for a sample of individuals captured at liftoff. In SBW–pyATM we express a moth's "flight strength" *s* as the inverse of the "wing load" (Rhainds, 2020), or:

$$s = A/M, \quad (5)$$

where *A* is the area of a single SBW forewing in [cm^2] and *M* is the moth's dry mass in [mg]. A moth with a large wing area and small mass would be considered a strong flier and should achieve a greater wind-relative flight speed than one with a small wing area and large mass. At a given wingbeat frequency (determined by temperature), each wingbeat thus counts more in terms of flight speed for the strong flier than for the weak flier. Given approximately normal distributions of wing area and mass for both male and female SBW (Régnière et al., 2019c), the distributions of flight strength *s* for males and females are also approximately normal with mean values slightly greater for males than for female moths (Fig. S5). A newly mated SBW female with a full complement of eggs is usually too heavy to lift off from the forest canopy (Régnière, 1983; Rhainds and Kettela, 2013), but her flight strength increases with weight loss due to oviposition and, given favorable conditions, her likelihood for liftoff increases over her life span (Rhainds, 2020). On the other hand, and discounting metabolic mass losses, we expect male SBW moths to maintain a relatively constant flight strength throughout their modeled dispersal period.

In our formulation of vertical flight speed, we have replaced the fixed α coefficient in Eq. (4) with the morphological flight strength *s* from Eq. (5) and a coefficient ε that represents the conversion of a wingbeat to actual moth propulsion:

$$v_z = \varepsilon\, s\, [\nu(T) - \nu_s], \quad (6)$$

where we assume ε is a constant characteristic of SBW morphology with units of [m s^{-1} mg cm^{-2} Hz^{-1}]. For dynamical consistency, we have also applied these wingbeat coefficient and flight strength factors to the calculation of horizontal flight speed:

$$v_h = -\,\varepsilon\, s\, \nu(T), \quad (7)$$

where all terms on the right side have the same values (for an individual moth) and units as in Eq. (6). While the values of ε, *s*, and $\nu(T)$ are always positive, we have found in comparisons with radar-based observations that $v_h > 0$ is unlikely; moths in flight appear to move more slowly than the wind, seemingly resisting the environmental wind while simply trying to remain aloft, leading to the negative sign in Eq. (7). Based on comparisons between simulated spatial concentrations of airborne moths and XAM radar observations at concurrent times, we have determined that $\varepsilon = 1.58$ m s^{-1} mg cm^{-2} Hz^{-1} as will be shown in Part 2 of this work.

Under normal conditions with an adequate boundary layer wind, the moth's ground-relative speed remains positive in the downwind direction, as suggested by Eq. (3). However, the moth can also move under its own power; if the flying moth enters an area of calm winds (as described above), it can continue its forward motion relative to the ground, instead of appearing to fly backward as strictly suggested by the combination of Eq. (3) with Eq. (7). We therefore amend Eq. (3) as

$$v_{h,g} = \max\,[(V_h + v_h),\ 1.0], \quad (8)$$

which allows for a minimum ground-relative forward speed of 1 m/s in otherwise calm wind conditions.

Landing phase: Of the three phases of moth flight described and modeled for this work, the landing phase is that for which we know the least from empirical observations. However, we can make several deductions based on physical considerations that are useful to our flight modeling activity. Moths in flight can be forced to descend and land because of rainfall, downdrafts, or temperature-dependent limitations on flight activity. Given the complex topography in our study region (Fig. S3) and the potential for large variability in vertical velocity, moths will sometimes land directly from the dispersal phase of flight without an explicit transition through a descent phase. The landing phase is defined as either (1) the point in time when the flight path of a moth intersects the forest canopy or the ground or water surface, or (2) when an external factor (such as low temperature or daylight) initiates landing behavior, characterized by a moth folding its wings and dropping out of the air. We consider most of these landings as harmless interruptions in the dispersal flight, except for drowning upon landing in water, and the moth can lift off from its new location again in the same night if suitable conditions occur.

There are three primary factors that can lead to moth landings without subsequent opportunities for re-flight in the same night. First, moths can be caught in a rainstorm and "washed out" of their flights by collision with raindrops and entrainment in downdrafts. For washout during flight, we apply the same precipitation rate threshold that would prevent liftoff of a stationary moth in the forest canopy, currently assumed as $R_{max} = 2.5$ mm/h. Second, the temperature at all altitudes may fall below the temperature threshold for SBW wingbeat activity ($T_{min} = 15$ °C; Sanders et al., 1978; Régnière et al., 2019c). Finally, we force any moths still flying at sunrise to initiate landing, consistent with observations by Greenbank et al. (1980). Regardless of the cause, simulated moths explicitly transitioning to the landing phase are programmed to descend with wings folded at the terminal fall speed assumed by Sturtevant et al. (2013), such that $v_z \in N(-2.0, 1.0)$ m/s and

$v_h = 0$ (drifting on the horizontal wind).

Gravidity and egg deposition: Our SBW–pyATM model distinguishes the sex of SBW moths and uses separate empirical distributions of morphological characteristics as given by Régnière et al. (2019c). Among the most distinguishing physical characteristics of SBW moths is gravidity, defined as the remaining proportion of the full natal fecundity carried by female moths. Female gravidity $G = F / F_0 = 1$ at eclosion, where F_0 is the moth's natal fecundity, and decreases with egg-laying opportunities over the female's life. Most female SBW with $G = 1$ are too heavy to fly even in summer evening conditions (Régnière, 1983; Rhainds and Kettela, 2013), so a female SBW typically lays about half of her initial egg complement at the natal site (improving her flight strength) prior to attempting dispersal flight. The female then lays about half of her remaining eggs at each subsequent landing site with a suitable host tree (Régnière, 1983; Rhainds and Kettela, 2013; Rhainds, 2020). This cycle continues until $G \leq 0.01$, indicating typically that the female has fewer than three eggs remaining, at which point the female moth is considered spent and is removed from the simulation.

3.4. Computation

In the results shown below, each night's flight simulation ensemble contains 1 M moths, covering 1000 replicate simulations using the same WRF-derived input and flight parameters and with each replicate using a random selection of 1000 SBW moths from BioSIM output for the 2013 SBW adult eclosion period (Fig. S4). The SBW moth is not a social or swarming insect, and there is no evidence to suggest that moths communicate or cooperate with each other during dispersal, such that the modeled SBW moths do not interact with each other during the flight simulation. This renders the ensemble simulation replicates linearly separable: independent replicates vary only in the initial locations and morphology of the moths themselves, while all other variables and flight parameters remain the same across the ensemble. The SBW–pyATM model framework thus lends itself to a distributed computational approach to each ensemble experiment, combining simulation results across numerous (100–1000) replicates to illustrate a dispersal flight event much larger than single-processor resources would reasonably allow. For model computations, we have employed clustered high-performance and distributed high-throughput computing systems at the University of Wisconsin–Madison and on the Open Science Grid (see Acknowledgements for links and references).

4. Results

We present here the results of SBW dispersal flight simulation ensembles covering southern Quebec and adjacent areas for the nights of 14–15 July and 15–16 July 2013. For each night, as the circadian flight readiness of the moths increases around sunset and into the evening, meteorological conditions favorable to moth liftoff and flight gradually deteriorate, with the result that not all 1 M moths initialized for each night engage in dispersal flight. Summary flight statistics derived from each night's simulation ensemble are listed in Table 1. Note that simulation times are given in UTC (Coordinated Universal Time) and that, in our study area, local daylight time (LDT) = UTC – 4 h. Thus, for example, 00 UTC on 15 July = 20 LDT on 14 July, shortly before sunset in our study area.

4.1. Weather conditions and simulated SBW dispersal patterns on 14–15 July 2013

The weather in our study area is marked by warm daytime conditions and moderate winds on the first night of these simulations (Figs. 3 and S6). As simulated SBW flight altitudes generally range from near the surface up to ~1.5 km above ground level (AGL), we have chosen to illustrate flight-relevant meteorological conditions with the wind speeds at 900 hPa, typically ~1 km above mean sea level (AMSL), and the surface temperatures. At 00 UTC on 15 July, just prior to sunset (~08 LDT on 14 July), westerly winds in the range of 5–12 m/s are present at 900 hPa (Fig. 3a) with generally light winds at canopy level (Fig. 3c). Through the night, the flight-level winds generally increase with time and turn to a northwesterly direction (Fig. 3b) and surface temperatures decrease slowly by 06 UTC on 15 July (Fig. 3d), several hours before sunrise (typically at ~09 UTC, ~05 LDT). Beginning around sunset (Fig. S7), large numbers of SBW moths disperse primarily from the St. Jean Lake region of central Quebec (see Fig. 1) to the east and southeast, many crossing the St. Lawrence estuary (Fig. 4). With higher topography between the St. Jean Lake area and the estuary (Fig. S2), many SBW moths fly only a short distance before landing in the mountains on the northeast side of the Saguenay River. Other SBW moths either skirt this higher topography with a more eastward course or fly high enough to pass over it, after which a great number land in the estuary itself. Of those moths that cross the estuary to land, most SBW landings on this night occur in the Lower St. Lawrence and Gaspe regions of Quebec, in northern New Brunswick, and in northern Maine (Fig. 4).

Nearly 60% of the 1 M moths initialized for this simulation ensemble engage in dispersal flights, with more than 85% males and only 15%

Table 1
Summary SBW dispersal flight statistics for the 14–15 July and 15–16 July 2013 simulation ensembles. Note that the percentages of individual sexes in the "fliers" and "non-fliers" categories add up to 100% of moths in the respective category, while the overall percentages of moths in those categories add up to 100% of all moths in the collected simulation replicates.

Simulation Date		14–15 July 2013			15–16 July 2013		
Sex		Male	Female	Overall	Male	Female	Overall
Fraction							
	non-fliers	23.4%	76.6%	41.2%	33.4%	66.6%	51.6%
	fliers	85.2%	14.8%	58.8%	87.5%	12.5%	48.4%
	all moths	59.8%	40.2%	100.0%	59.6%	40.4%	100.0%
Flight altitude (m AGL)							
	mean	818	440	762	679	315	634
	st. dev.	223	153	252	190	160	222
	mean of max.	1167	722	1101	958	509	902
Flight duration (mins)							
	mean	443	276	418	410	218	386
	st. dev.	116	146	135	135	118	148
	max.	716	662	716	726	648	726
Flight distance (km)							
	mean	185	138	178	120	89	116
	st. dev.	58	86	65	50	63	53
	max.	329	358	358	359	368	368

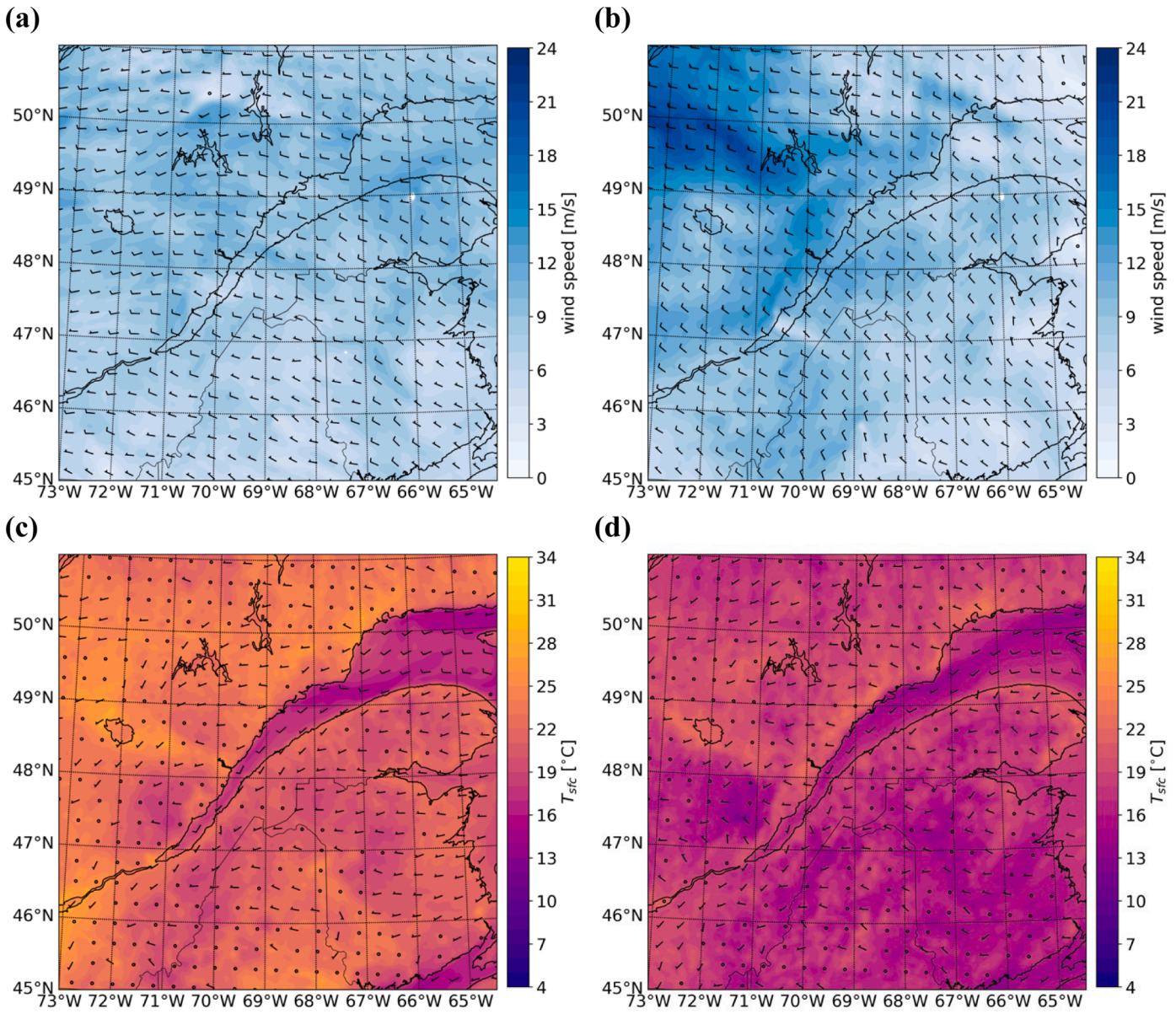

Fig. 3. WRF-based regional weather maps for the 14–15 July 2013 dispersal simulation: (a,b) wind speed (m/s, colored) and wind barbs at 900 hPa; (c,d) temperature (°C, colored) and wind barbs at the surface; (a,c) at 00 UTC on 15 July 2013; (b,d) at 06 UTC on 15 July 2013. Additional weather conditions through the night are provided in Fig. S6. An animation of these weather conditions through the night is available in the Supplemental Materials.

females (Table 1). Males demonstrate greater simulated flight durations and distances than females, though females exhibit greater variance in both of those measures. Males generally fly higher than females, with the mean simulated male flight altitude just over 800 m AGL, while simulated female flights have a mean altitude of just 440 m AGL and less variation (Table 1).

Part of this work is oriented toward the validation of simulated SBW flight patterns with available XAM radar observations during the study nights. Simulated concentrations of SBW moths within the XAM coverage area are generally low, given that our model represents just a bare fraction of the actual dispersing SBW population on a given night. Our method for quantitative comparison that accounts for such differences will be shown in Part 2 of this work. For the purposes of this paper, our simulated patterns of moth flights are generally consistent with areas of greater radar reflectivity at the same time (Fig. 5). Overall, higher concentrations of simulated moths match greater values of radar reflectivity on the north side of the St. Lawrence estuary near the North Shore early in the night (Fig. 5a,b). Later in the night, our simulated moth concentrations do not correspond as well with the areas of greatest radar reflectivity, especially along a line of apparent low-level wind convergence over the estuary (Fig. 5c,d), though the flight model does suggest a large concentration of water landings by SBW males in that vicinity (Fig. S8b).

4.2. Weather conditions and simulated SBW dispersal patterns on 15–16 July 2013

Our SBW–pyATM simulations demonstrate a significantly different spatiotemporal pattern of moth dispersal on the second night of this study, with warmer surface and boundary layer temperatures throughout the night of 15–16 July 2013 (Figs. 6 and S11). This night begins with stronger winds at 9–15 m/s from the northwest just prior to sunset (Fig. 6a) that weaken slightly and turn to the north through the night (Fig. 6b). The simulated pattern of SBW liftoff times (Fig. S11) and flights (Fig. 7) suggest several differences from the previous night. First, liftoff times are concentrated primarily in the pre-sunset period, as

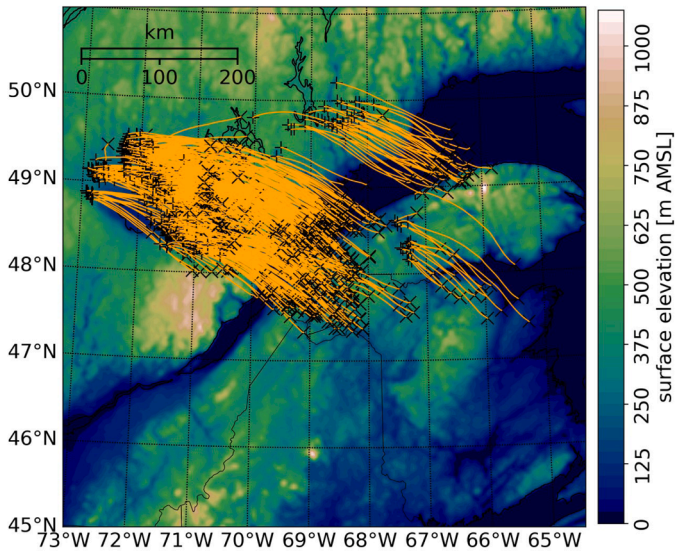

Fig. 4. Regional topography with simulated 14–15 July 2013 SBW moth flight trajectories. These trajectories are from a single 1000-moth replicate in the overall simulation ensemble. Liftoff and landing locations are denoted with "+" and "×" signs, respectively. An animation of SBW moth dispersal through the night is available in the Supplemental Materials.

compared with the previous night, reflecting a faster rate of near-surface cooling just after sunset where most of the moths are ready to lift off. Second, instead of flying generally eastward, the large number of simulated SBW moths initiated in the vicinity of St. Jean Lake are funneled by the northwesterly flow toward the Saguenay River valley, where many of their flights intersect with the high terrain on both sides of the valley. Some of the simulated SBW flights negotiate the valley passage, turn south, and eventually cross the estuary to land in areas south of the St. Lawrence estuary in Quebec and farther into northern Maine than dispersing moths reached on the previous night. Simulated SBW moths initiated in the North Shore area lift off to fly directly south, but many turn sharply to the southwest once over the St. Lawrence estuary and eventually land in the water. A few of those simulated North Shore moths cross the estuary to reach areas of Lower St. Lawrence, northern New Brunswick, and northern Maine by the end of their flight. The persistent northerly winds over areas south of the estuary carry some SBW moths initiated in the Gaspe region southward to land well into New Brunswick by the end of the night.

On the night of 15–16 July 2013 fewer than 50% of the modeled SBW adult moths attempt dispersal flights, likely as more rapid near-surface cooling after sunset reduces the possibility of later flights, with males again constituting the overwhelming fraction (~88%) of the migrants. Of those simulated moths that attempt to fly, again it is the SBW males that generally demonstrate longer and higher flights, though these values are smaller than on the previous night. Overall, in this second night's simulation ensemble both males and females fly only two-thirds as far as on the previous night, and both sexes fly at lower altitudes during their dispersal attempts.

Radar observations of SBW movement within the XAM coverage area during the night of 15–16 July 2013 were examined in detail by Boulanger et al. (2017). Our modeled dispersal flights on 15,16 July indicate good correspondence between simulated SBW concentrations and greater values of radar reflectivity in the vicinity of the St. Lawrence estuary (Fig. 8). Early in the night, a counterclockwise swirling feature appears in the low-level wind field just southeast of the North Shore and propagates upstream (to the southwest) along the northern side of the estuary. This feature is clearly visible in the radar observation at 0159 UTC (Fig. 8b) and is reflected in the sharp right turn of SBW migrants leaving the North Shore region (Fig. 7). By 0359 UTC, our simulated concentrations of SBW migrants over the St. Lawrence estuary (Fig. 8c) correspond well with that feature's transition to a near-linear low-level convergence zone (Fig. 8d).

4.3. Simulated individual and aggregate flight behavior

Individual SBW flight profiles in our simulations are consistent with the programmed physiological responses to the environmental temperature. The moths lift off in warm conditions, ascend quickly to altitudes at which their dispersal is supported by strong winds, and then land at various times during the night in relatively cool conditions as either their trajectories intersect the topography or sunrise occurs. Between the liftoff and landing phases of flight, the behavior of each moth is dictated by the environmental temperature and detailed model outputs allow us to examine individual flight profiles over the course of each night (Fig. 9). These flight profiles indicate that moth flight over complex terrain is strongly affected by both temperature and topographic influences on vertical wind patterns, though not necessarily in equal measure, and that a moth's flight altitude varies frequently in response to these influences.

To supplement our examinations of dispersal weather conditions given above, and to illustrate the correspondence between simulated SBW flight behavior and specific environmental conditions, we also examine hourly time series of WRF-derived temperature and wind speed vertical profiles on each night (Fig. 10) at locations where large numbers of simulated moths cross the St. Lawrence estuary (see markers in Fig. 1). A clear correspondence between temperature and wind profiles for the night of 14–15 July 2013 (Fig. 10a) and simulated flight altitude distributions (Fig. 11a) indicate that flying males concentrate in the layer where the vertical temperature gradient is strongest over much of the night, which is also the layer where the horizontal wind speed is greatest. This factor, combined with longer simulated flight times for most males than for females (Table 1), leads to far greater distances traveled by males on the first night. Simulated flights of dispersing females concentrate in a lower and generally warmer layer where lesser wind speeds occur over the night (Fig. 10a). These differences in flight altitudes and durations are reflected in the distributions of flight distance during the 14–15 July 2013 dispersal event (Fig. 11b). It is interesting to note that the simulated flight distances for female SBW peak at less than 100 km but that the distribution is spread over all distances between 50 and 300 km, with a minor peak at 300 km representing long-flying females forced to land at sunrise. Simulated male flight distances have a distribution peak near 240 km, a distance that is greater than the overall mean for males (185 km).

During the 15–16 July 2013 dispersal event, similar relationships apply between the temperature and wind profiles (Fig. 10b) and the simulated distributions of flight altitude (Fig. 11a) but with far different results for simulated flight distances (Fig. 11b). The modeled SBW liftoff period ends earlier (Fig. S11) than during the previous evening, and flight durations on this second study night are somewhat shorter (Table 1). Simulated mean flight distances for each sex are smaller than those on the previous night by nearly one-third. The distributions in Fig. 11b for 15–16 July show a sharp peak in simulated male flight distances near 100 km, slightly less than the overall mean flight distance for males on that night (120 km), but with a long tail in the distribution out to approximately 300 km. Simulated female SBW dispersal on this second night exhibits a bimodal distribution of flight distances, with maxima at ~40 and ~120 km on either side of the overall mean female flight distance (89 km; Table 1) and a much shorter distribution tail (~200 km) than for females on the first study night (~300 km).

4.4. Spatial patterns of egg deposition, male landings, and transported fecundity

Simulated liftoff and landing locations for both sexes are shown for each night in this study, respectively, in Figs. S8 and S13 for males, and

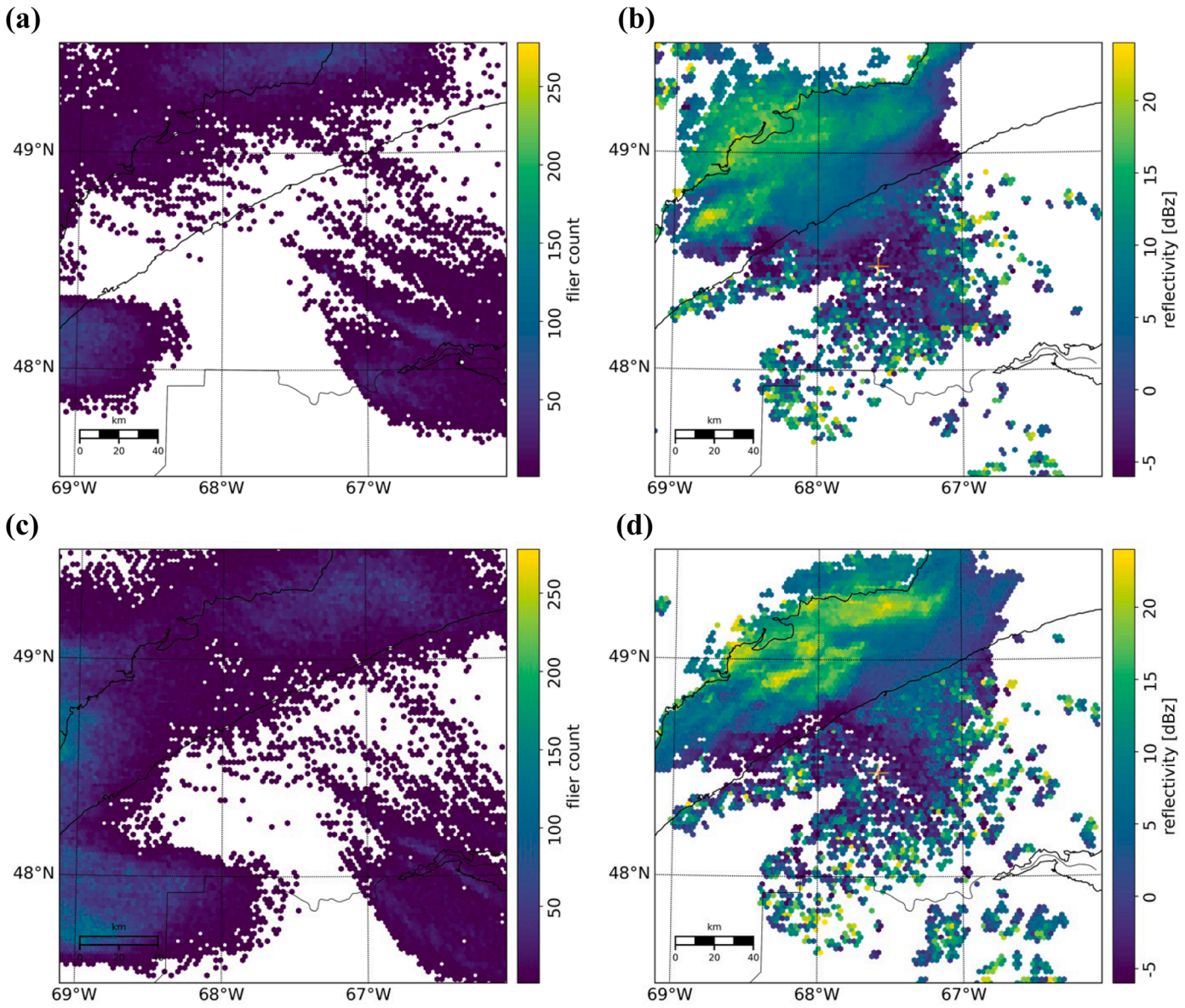

Fig. 5. (a,c) Simulated spatial concentrations of SBW moths compared with (b,d) XAM radar observations at (a,b) 0429 UTC on 15 July and (c,d) 0629 UTC on 15 July during the 14–15 July 2013 dispersal event. An animation of this comparison through the night is available in the Supplemental Materials.

Figs. S9 and S14 for females. Maps of natal-site oviposition (Fig. 12a,c) resemble those of simulated fecundity export (Figs. S10a and S15a), which in turn resemble the maps of modeled female liftoff counts (Figs. S9a and S14a) weighted according to the remaining fecundity of the emigrating females. Maps of simulated fecundity import for immigration locations on 14–15 July 2013 (Figs. 12b and S10b) and on 15–16 July 2013 (Figs. 12d and S15b) are thus similar in spatial pattern to the maps of simulated female landing counts (Figs. S9b and S14b), and the simulated patterns of male landings (Fig. 12b,d) are reproduced from the modeled ensemble concentrations in Figs. S8b and S13b.

5. Discussion

5.1. Modeled SBW flight dynamics

Our SBW–pyATM simulations of dispersal flight events focus on the responses of individual, morphologically distinct SBW moths to their environment as temperature and wind conditions change over a given night. The SBW–pyATM framework compiles the collective behavior of large numbers of modeled individuals via simulation ensembles driven by regional weather model outputs based on historical reanalysis data. The simulated spatiotemporal patterns of SBW dispersal and fecundity transport generated by our model framework thus emerge from rapidly changing environmental conditions in the atmospheric boundary layer and their combination with empirically described SBW behaviors. Dispersal distances and spatial patterns are sensitive to mesoscale weather conditions that evolve within single nights and large-scale synoptic patterns that can change significantly from one night to the next. Over several weeks each summer, the accumulated spatial patterns of SBW flights are critical to our understanding of dispersal behavior and its consequences on outbreak evolution at larger spatial scales and longer time scales, from years to decades.

In the SBW–pyATM framework, our dispersal flight model investigates and represents individuality in SBW flight behavior by accounting for the variations in flight capacity between moths based primarily on body mass and wing size. Several studies of agricultural pest dispersal have used the NOAA HYSPLIT model (Stein et al., 2015), including the work of Westbrook et al. (2016, 2019) on fall armyworms and that of Wang et al. (2019, 2021) and Koralewski et al. (2021) on sugarcane aphids. Others (*e.g.*, Zhang et al., 2018) addressed the

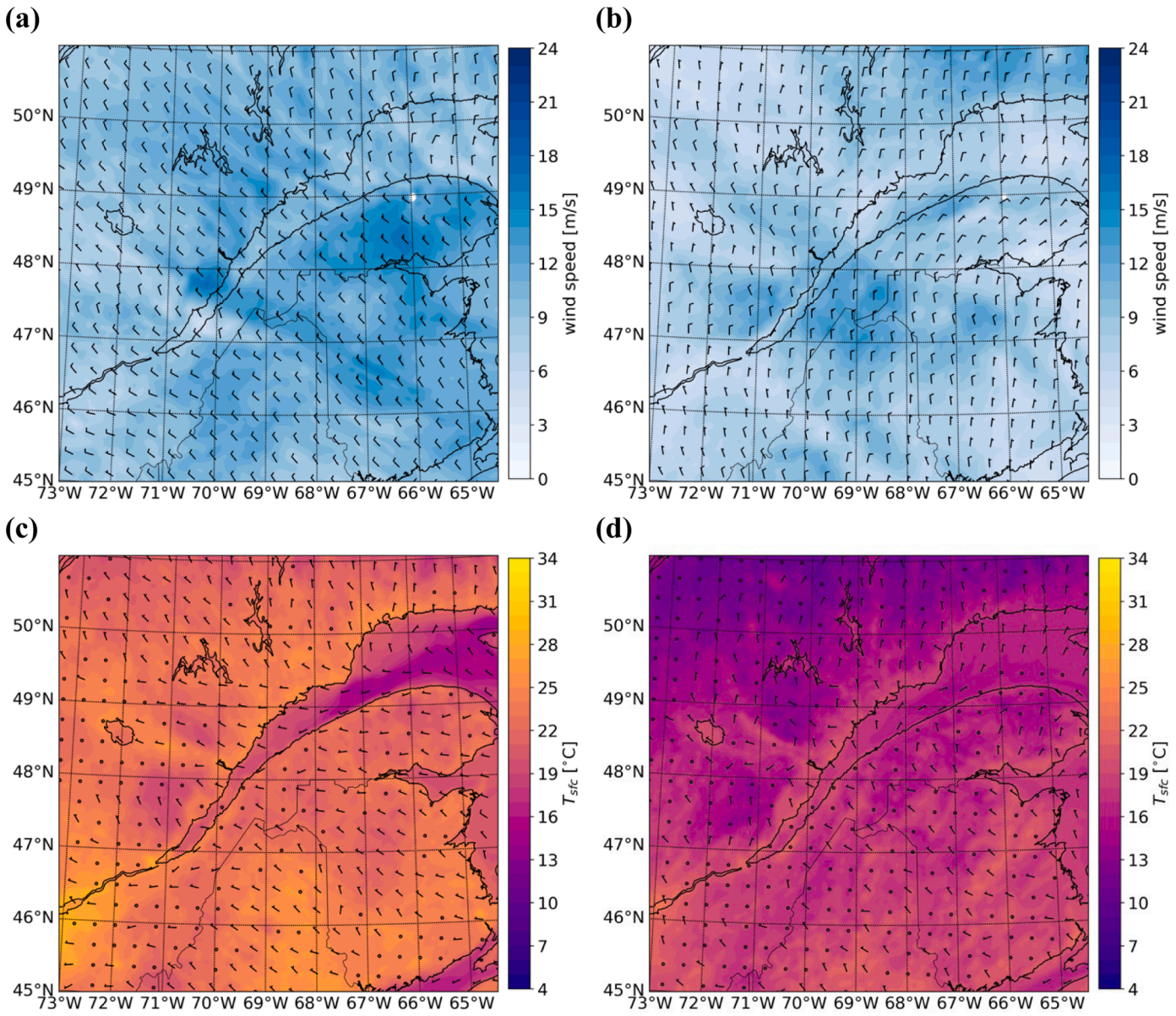

Fig. 6. WRF-based regional weather maps for the 15–16 July 2013 dispersal simulation: (a,b) wind speed (m/s, colored) and wind barbs at 900 hPa; (c,d) temperature (°C, colored) and wind barbs at the surface; (a,c) at 00 UTC on 16 July 2013; (b,d) at 06 UTC on 16 July 2013. Additional weather maps through the night are provided in Fig. S11. An animation of these weather conditions through the night is available in the Supplemental Materials.

migration of fall armyworms in Asia using the FLEXPART model (Stohl et al., 2005). These studies with HYSPLIT and FLEXPART all used the Weather Research and Forecasting (WRF) model (Skamarock and Klemp, 2008; Skamarock et al., 2008; Powers, 2017) to generate high-resolution meteorological conditions that drive the calculated insect dispersal. We also use WRF input here. However, neither HYSPLIT nor FLEXPART allows true "agency" to the dispersed particles, treating them as inert (or, perhaps, only chemically reactive) tracers that move with the wind. Those studies have all required the initial specification of dispersal source location and height in the atmosphere, from which the insects or tracers proceed by Lagrangian calculation to their eventual landing locations, often after a specified flight duration. For modeling SBW dispersal, we use explicit descriptions of individual SBW liftoff and flight behavior that obviate the specification or imposition of such initial conditions and physical passivity on dispersal flight timing, altitude, and path.

In SBW–pyATM, incorporating the circadian rhythm of SBW flight activity (Régnière et al., 2019d) and a detailed physiological model of temperature-based flight behavior (Régnière et al., 2019c) has made our simulated liftoff timing (Figs. S7 and S12) and flight altitudes (Figs. 9 and 11a) more dynamic and realistic than those simulated in prior work. The resulting maps and vertical profiles of moth concentration are qualitatively in agreement with radar observations of dispersal flights on the examined nights. Future work will address these comparisons quantitatively as part of our model calibration process, and additional analyses will address the relative consistency of the timing and extent of simulated flight patterns with empirical ground-based samples of SBW moth activity.

Our individual-based SBW–pyATM simulation results suggest that the outcomes of a single dispersal event including flight timing, distances, and overall spatial patterns of emigration and immigration can differ substantially by sex. Male SBW are generally lighter than females and, according to our model results, fly higher and farther than the SBW females (Fig. 11; Table 1). For SBW females, the burden of fecundity strongly limits lift-off rates and timing, flight altitude and duration, and thus flight range. Both males and females may survive for multiple

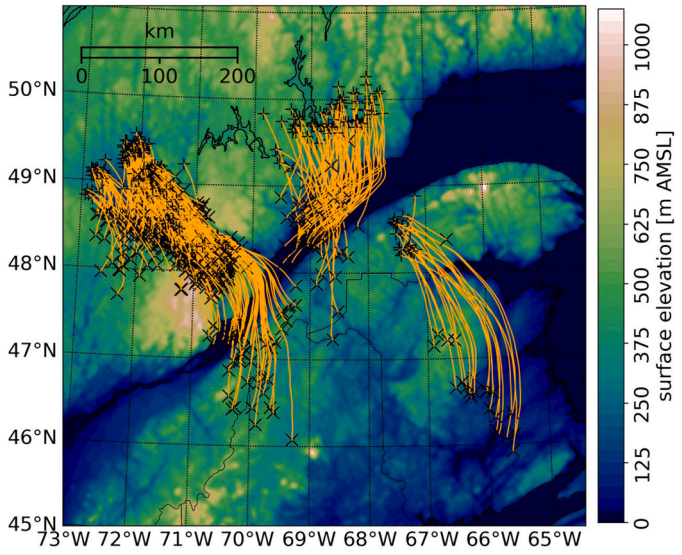

Fig. 7. Regional topography with simulated 15–16 July 2013 SBW moth flight trajectories. These trajectories are from a single 1000-moth replicate in the overall simulation ensemble. Liftoff and landing locations are denoted with "+" and "×" signs, respectively. An animation of SBW moth dispersal through the night is available in the Supplemental Materials.

flights over several nights; previous work has suggested that SBW females may proceed through egg deposition and onward flights over successive days and nights, respectively (Miller et al., 1978), and SBW males immigrating at the time of local female eclosion may help overcome limits to mating success (Contarini et al., 2009; Tobin et al., 2009; Rhainds, 2010; Régnière et al., 2013). Our dispersal model results suggest that male and female SBW may carry out their respective roles in the development and continuation of outbreak conditions in vastly different locations following each night over the dispersal period, and such differences can have significant consequences for the spatiotemporal patterns of SBW mating, dispersal, and egg deposition leading to the next generation of SBW larvae and moths. The simple filter of physiological individuality may lead to complex emergent patterns and dynamics in year-to-year outbreak activity that we may now be able to explain through the lens of SBW dispersal flight behavior.

5.2. Model contributions to understanding SBW outbreak dynamics

Régnière and Nealis (2019) described the roles of "source" and "sink" regions in the large area of an SBW outbreak. Our SBW–pyATM framework can help elucidate three of the major components of those population dynamics: (1) the potential for female emigration and fecundity export to limit the size of the next generation of SBW in source populations, (2) the role of female immigration and fecundity import to enhance the size of the next generation of SBW in sink populations, possibly pushing the local population over a density threshold to outbreak conditions, and (3) the potential for male immigration to help mitigate mating failure in SBW sink populations, also contributing to the potential transition to outbreak conditions at local scales.

Of these factors, the transport of SBW eggs and the patterns of immigrant fecundity are among the most theoretically important but least-clearly observed drivers of spatially distributed SBW population dynamics (Miller et al., 1978; Nealis and Régnière, 2004; Régnière and Nealis, 2007; Régnière et al., 2019a). Cumulative effects of seasonal moth dispersal can mitigate two of the primary Allee effects limiting the development of low-density SBW populations to outbreak levels: natural enemies (Nealis and Régnière, 2004; Régnière and Nealis, 2007; Régnière et al., 2019a) and, as mentioned above, mating failure (Régnière et al., 2013). The first can be overcome by the deposition of sufficient numbers of eggs by immigrant females that a large number escape predation, and the second factor can be overcome by the timely influx of males during local female eclosion in low-density populations.

Key to the usefulness of our individual-based, weather-driven, night-by-night accumulative modeling approach to SBW dispersal is this role of flight timing in the overall dynamics of the SBW outbreak. A location at which SBW adults emerge, mate, and lay their initial egg complement may or may not then experience environmental conditions conducive to dispersal within the female's life span. If flight conditions remain unfavorable and the females do not emigrate that year, they might find additional suitable host trees for further egg deposition in their immediate vicinity, but the potential for overcrowding may increase with consequences for spring food availability (Régnière and Nealis, 2007; 2019; Van Hezewijk et al., 2018), adult reproductive success (Delisle and Hardy, 1997), and the full realization of female fecundity (Queza-da-García and Bauce, 2013; Frago and Bauce, 2014) the next summer. If emigration does occur, the typical risks of dispersal apply: SBW females may or may not survive the flight and may or may not find suitable host trees at landing locations, and their progeny could be exposed to unfavorable weather conditions, could fall prey to predators and parasites, and could starve in a severely defoliated forest stand with diminished capacity for regrowth. On the other hand, it remains possible that the dispersal flight results in successful immigration at a new host forest location, and the next generation of SBW may flourish in a favorable habitat under ideal conditions. Our ability to estimate these landing locations and the resulting spatial patterns of egg distribution, combined with the SBW lifecycle modeling provided in BioSIM, will soon allow us to forecast larval defoliation activity and the potential for SBW population growth, perhaps to outbreak densities, in new locations.

5.3. Model limitations

Our SBW–pyATM framework represents an updated synthesis of what remains known and unknown regarding the aerobiology of SBW dispersal. Still, some aspects of the flight model remain uncertain. The model is sensitive to the uncertainties of its mathematical formulation: several rules for liftoff, flight, and landing have been specified with unknown or uncertain parameters governing their outcomes. We have identified and described these parameters in the Methods, and we have developed observation-based procedures to calibrate those parameter values that will be presented in future work. Additional uncertainties include the behaviors of SBW moths in the liftoff and, especially, the landing phases of flight. Unfortunately, to date we have detailed observations for only some of these uncertain behaviors to inform our programmed individual flight rules.

For example, at liftoff there are numerous influences on the SBW adult's "choice" to fly at all. Among these drivers is the local availability of food resources sufficient to support the next generation of SBW upon larval emergence the following spring. These are density-dependent aspects of SBW population dynamics that, while studied in detail in previous work (Royama, 1984; Régnière and Nealis, 2007, 2019; Van Hezewijk et al., 2018), we have not yet incorporated into our individual-based SBW modeling framework. An additional driver of the SBW moth's choice to lift off is the immediate environment itself: while we have addressed the diminished likelihood of flight in calm conditions, it is conceivable that SBW moths waiting in the forest canopy for ideal (or simply adequate) liftoff conditions are more likely to take advantage of wind gusts upon frontal passage (Dickison et al., 1983) and especially ahead of storm events (Dickison et al., 1986). Such behavior could serve several purposes: (1) remaining in the canopy through a rainstorm would delay subsequent liftoff attempts until the moth's wings have dried, (2) it is often the case that temperature and wind conditions following storm passage will be less favorable to liftoff, likely delaying emigration to another evening, and (3) liftoff in turbulent pre-storm gusts may carry the moth quickly above the forest canopy and far downwind, effectively extending the moth's flight range over that

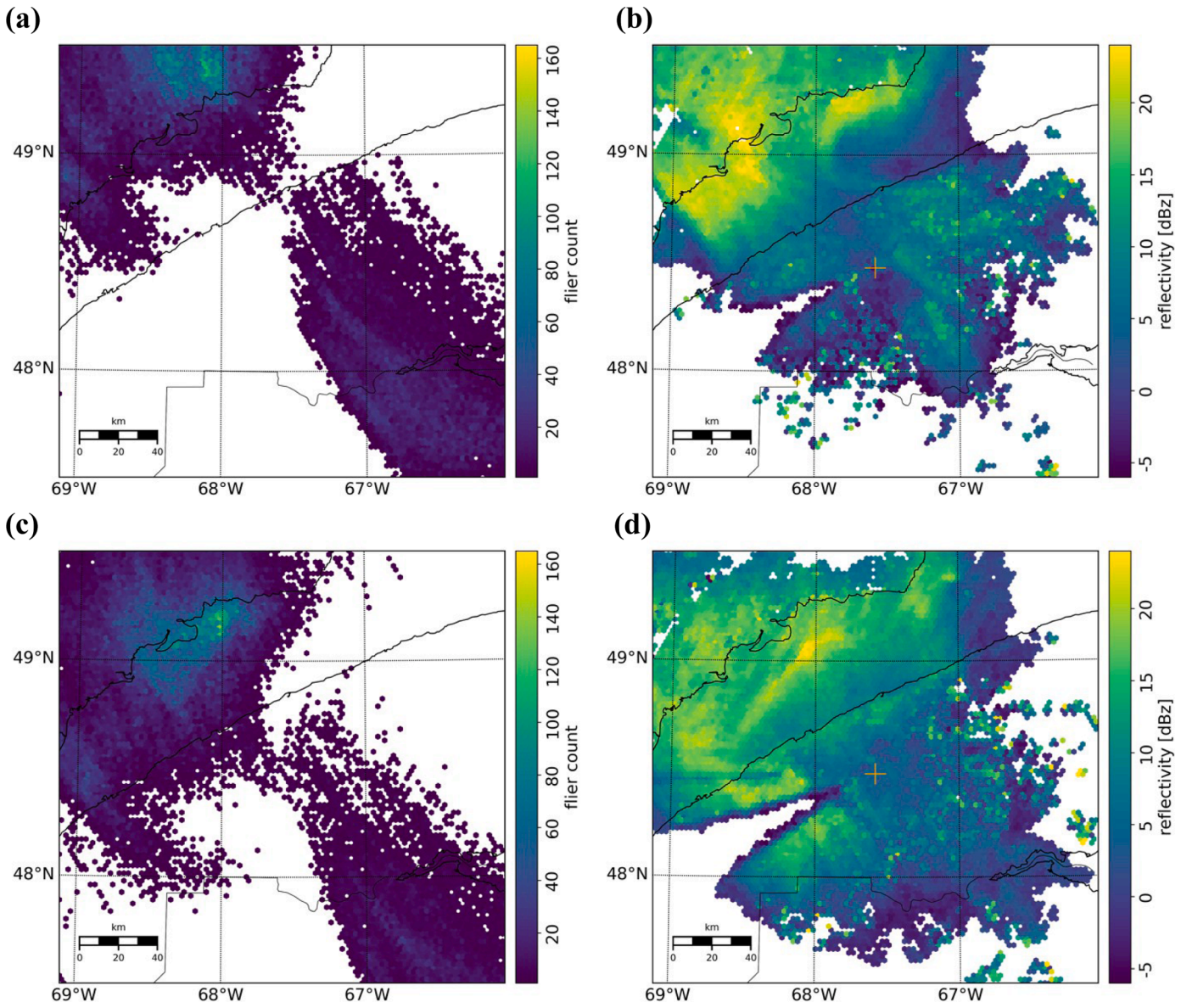

Fig. 8. (a,c) Simulated spatial concentrations of SBW moths compared with (b,d) XAM radar observations at (a,b) 0159 UTC on 16 July and (c,d) 0359 UTC on 16 July during the 15–16 July 2013 dispersal event. An animation of this comparison through the night is available in the Supplemental Materials.

night.

While in flight, storms such as those that could delay or prevent liftoff might also wash the flying moths out of the air. Greenbank et al. (1980) and Dickison et al. (1983, 1986) collected radar observations over New Brunswick and tracked SBW dispersal flights both with and without storms present, demonstrating that thunderstorms and precipitation cells can interrupt those flights. We have not yet addressed this possibility, primarily because radar observations indicated that it was not needed for the two nights examined here. However, ongoing investigations will introduce this consideration to our flight model and will allow us to examine additional dispersal flight events, in less favorable weather, in future work.

Landing behavior in SBW moths also remains highly uncertain, with even fewer available observations than for liftoff to guide our model ruleset. We have imposed some limitations on flight that lead to landing including sunrise (Greenbank et al., 1980) and precipitation (Greenbank et al., 1980; Dickison et al., 1983, 1986). We expect that the physiological dependence of wingbeat on temperature (Régnière et al., 2019c) leads to many simulated flight landings in the cooling nocturnal boundary layer, before the morning return to a warming (and turbulent) boundary layer condition. However, and again, we have not yet been able to address a key issue of apparent SBW choice: moths in flight may be able to sense the presence of host species in their path (*e.g.*, Sturtevant et al., 2013) and may even make an extra effort to reach land when flying over water. The question remains: how much influence do these cues assert on the moth's willingness to continue flight despite fatigue, or to steer its flight across the wind toward a more desirable landing location? Understanding such in-flight behaviors will greatly improve our ability to describe and simulate the various landing patterns in SBW moths.

Finally, as mentioned in the Methods, our initial use of the SBW–pyATM for simulating dispersal events over a single night carries several assumptions regarding the use of BioSIM output and imposes some limitations on interpretation and use of the results presented here. In ongoing work, we seek to remove those assumptions by having BioSIM and pyATM work in concert over several days and nights, and eventually a complete dispersal season. With a more tightly coupled modeling system, we will be able to simulate the activity of the SBW moths in "real-time" as they emerge from pupation, mate, deposit eggs in their natal location, disperse to find new favorable host trees, deposit

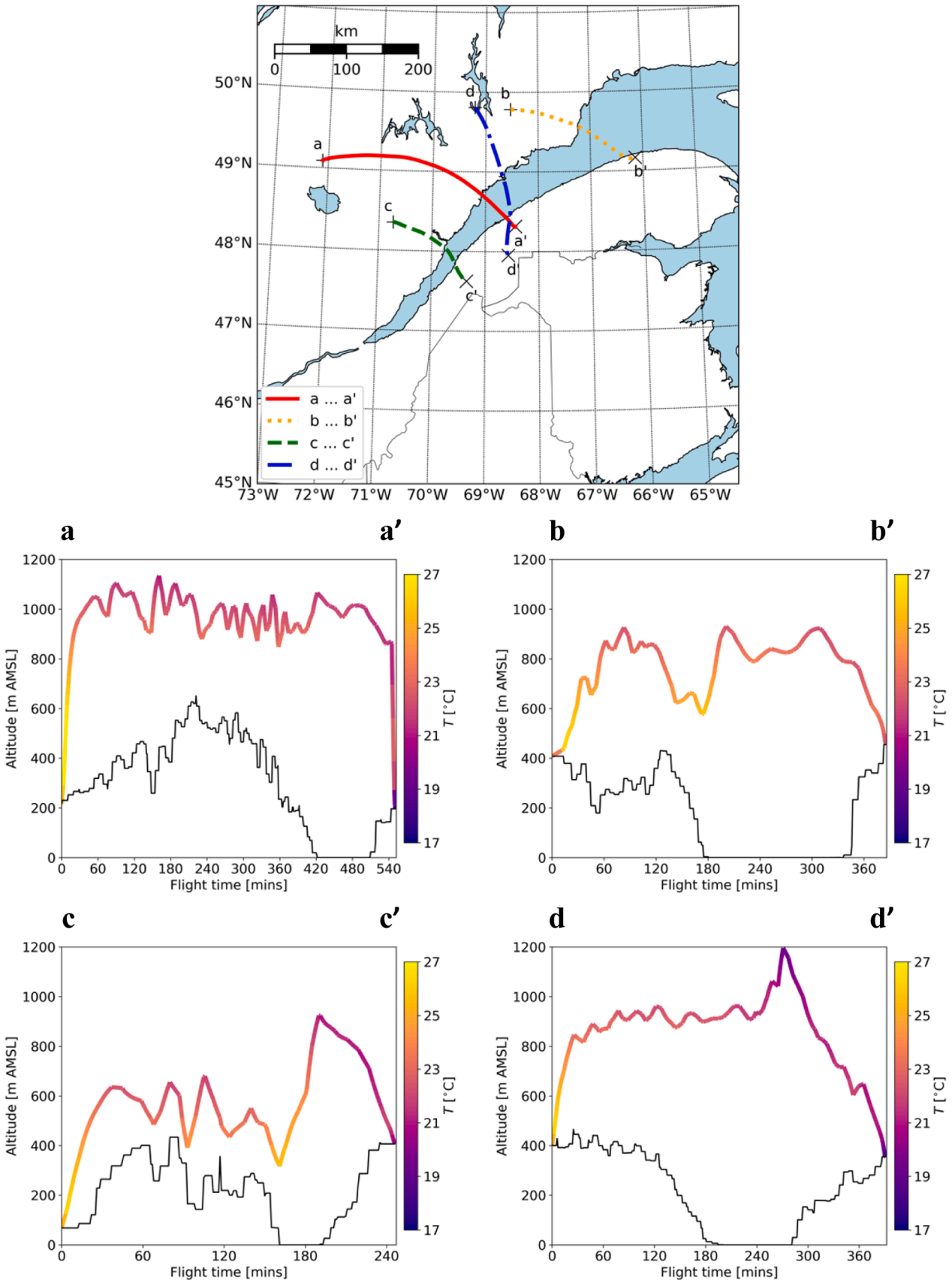

Fig. 9. Simulated dispersal flight trajectories and temperature/altitude profiles for selected individual SBW moths on (a,b) 14–15 July and (c,d) 15–16 July 2013. Liftoff ("+") and landing ("×") locations are denoted in the top panel. The bottom panels show the WRF-based ground surface elevation in black and the SBW flight altitude and environmental temperature in color, both with an exaggerated vertical scale.

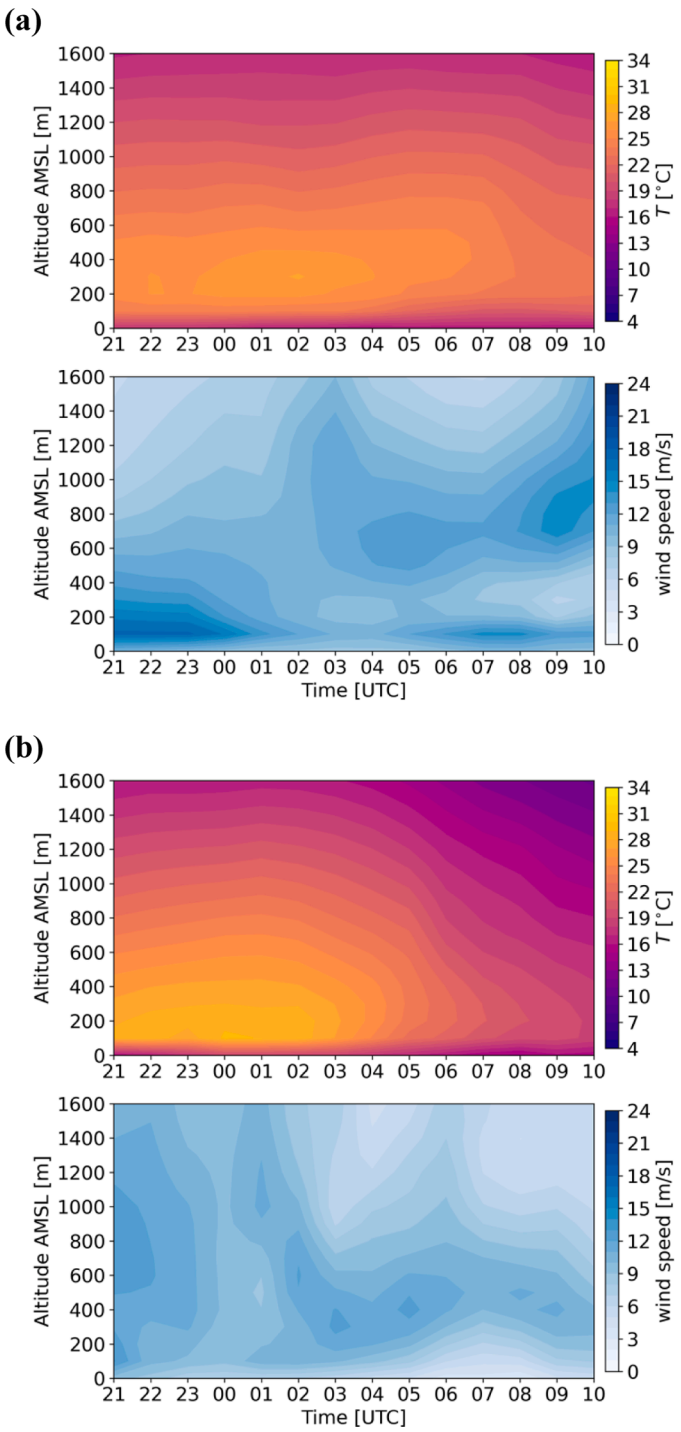

Fig. 10. WRF-based vertical profile time series of temperature and wind speed over the St. Lawrence estuary on (a) 14–15 July and (b) 15–16 July 2013 at the locations marked in Fig. 1.

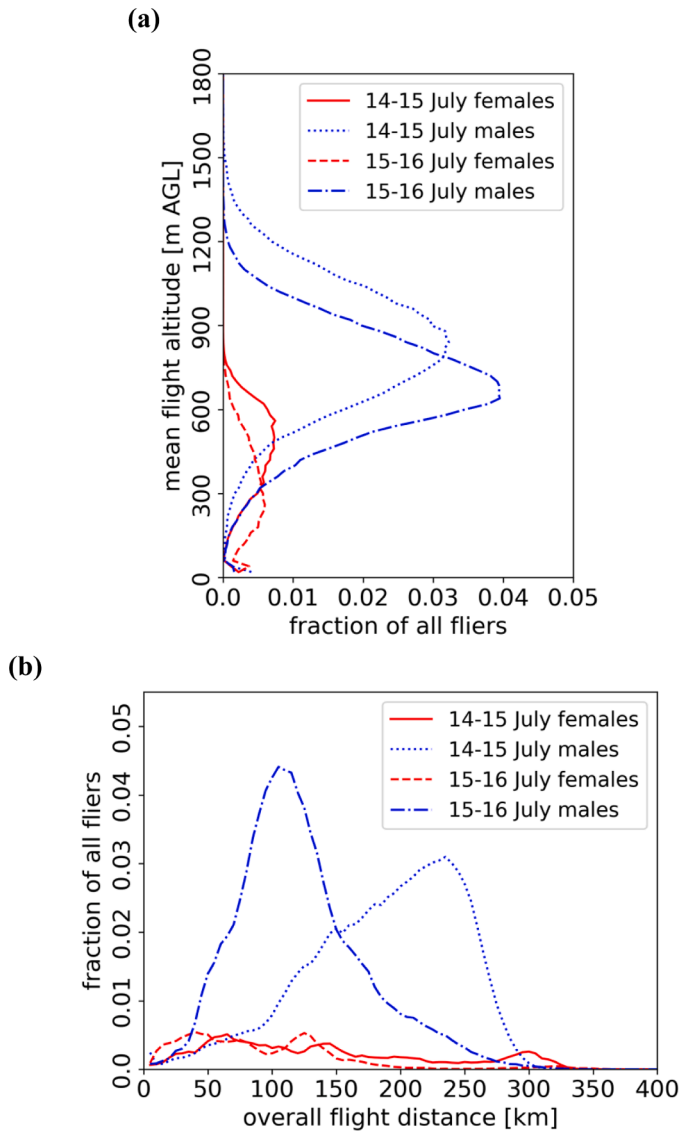

Fig. 11. Simulated SBW (a) mean flight altitudes and (b) flight distances for 14–15 July and 15–16 July 2013.

eggs again, and disperse again from that new location. We are working toward modeling this continuous daily cycle of reproductive activity and dispersal that will eventually provide more complete (and possibly more accurate) maps of SBW egg deposition throughout the outbreak region on a full-season basis, potentially supporting predictions of overwinter survival and spring defoliation activity the following year.

6. Conclusions

Above-canopy dispersal occurs during the adult life stage in SBW. Moth flight is driven primarily by weather conditions occurring over large areas and leading to mass dispersal events on a near-nightly basis in the warmest period of summer. Because SBW dispersal occurs during the egg-laying process, these dispersal events, both individually and aggregated over the season, may redistribute SBW populations leading to the spread of an outbreak. Locations of SBW outbreak populations and the resulting defoliation of host trees can change significantly from one year to the next.

Our SBW–pyATM dispersal simulations, even on a single-night basis, advance the representation of SBW outbreak evolution as an emergent phenomenon based on the behavior of countless individuals subject to a common ruleset under dynamic environmental conditions. This individual-based approach to dispersal flight modeling, while computationally intensive, remains flexible and extensible with numerous opportunities for new and novel diagnostic analyses, behavioral experiments, and applications of the results to the problem of SBW outbreak initiation, spread, and collapse in the boreal forests of eastern North America. Our modeling framework is likely generalizable to various insects including other forest defoliators and agricultural pests (*e.g.*, armyworms, aphids, possibly locusts), given sufficient empirical data on their dispersal aerobiology. Several ongoing research efforts will

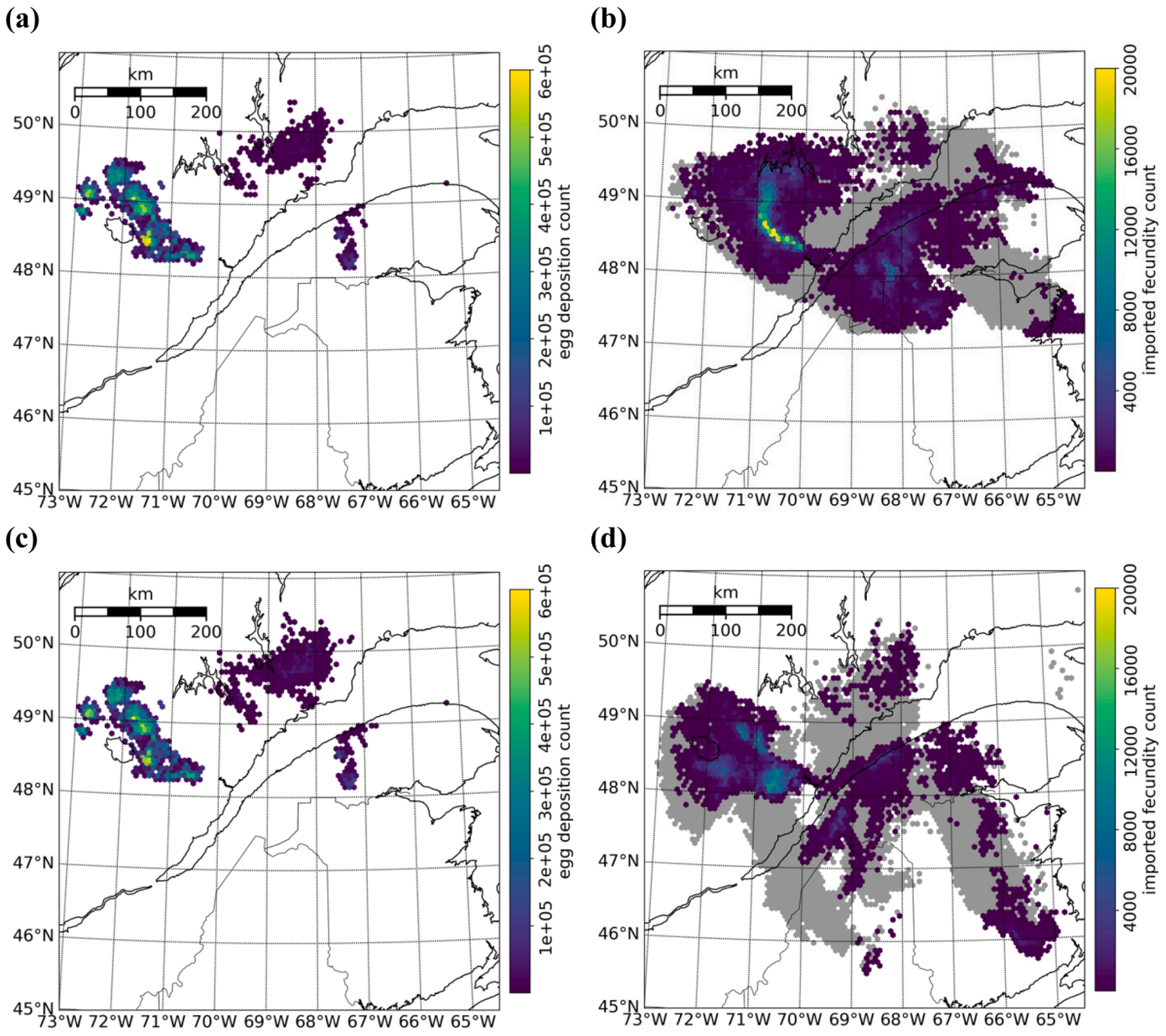

Fig. 12. Simulated (a,b) 14–15 July and (c,d) 15–16 July 2013 fields of (a,c) natal-site egg deposition and (b,d) male landing areas (in gray) and fecundity import by gravid SBW females (in color). Note the different color scales in each plot.

improve the numerous descriptions of SBW physiology and behavior included in the SBW–pyATM simulation framework. We aim to expand the physiological description of SBW flight with studies of metabolic energy storage and consumption and a physics-based model of moth flight. A better understanding of the rules affecting landing behavior will affect model outcomes regarding flight duration with potentially significant consequences for the spatial distribution of both male and female SBW landing locations.

Our SBW dispersal flight simulation results suggest that the two sexes are unlikely to perform their respective roles in the same locations and at the same time over the course of the dispersal season. Therefore, in ongoing work we aim to develop two specific metrics related to the spatiotemporal progression of SBW outbreaks: for SBW females, we are interested in simulated cumulative patterns and concentrations of oviposition through successive dispersal flights over multiple nights; for SBW males, we want to discern immigration patterns and concentrations relative to the timing of adult emergence in the local female populations, in the days *before* those gravid females would then depart on their own dispersal flights. As we expand model operations to longer periods, with the potential for individual SBW to fly again on successive nights and the consequent geographical expansion of imported fecundity and male immigration, we will be working toward individual-based simulations of full-season dispersal to better understand the emergent spatiotemporal distributions of SBW populations.

Code availability

Our SBW–pyATM software for individual-based flight simulations is available under the GPLv3 license at https://github.com/megarcia/SBW-pyATM. Python scripts and data used to generate the figures in this paper are available at https://github.com/megarcia/Garcia_etal_2022a. Sample datasets are available on Dryad at doi:10.5061/dryad.mpg4f4r19, and the supplemental animations are available on Zenodo at doi:10.5281/zenodo.5534999.

Declaration of Competing Interest

The authors declare that they have no known competing financial interests or personal relationships that could have appeared to influence the work reported in this paper.

Acknowledgments

We acknowledge Barry Cooke of the Canadian Forest Service for his contributions to the early stages of this project. We thank Frédéric Fabry at the J.S. Marshall Observatory, McGill University, for processing the radar data used here. We also thank U.S. Forest Service colleagues Susan Crocker and Andrew Liebhold for their comments on an earlier version of this manuscript, and two anonymous reviewers and the editor for their helpful comments during the review process.

We gratefully acknowledge the research computing facilitators, resources, and assistance of the UW–Madison Center for High Throughput Computing (CHTC) in the Department of Computer Sciences. The CHTC is supported by UW–Madison, the Advanced Computing Initiative, the Wisconsin Alumni Research Foundation, the Wisconsin Institutes for Discovery, and the National Science Foundation. The CHTC is an active member of the Open Science Grid, which is supported by the National Science Foundation (Award #2030508) and the U.S. Department of Energy, Office of Science.

Funding and additional resources directly supporting this work were provided by the U.S. Endowment for Forestry and Communities, the U.S.–Canadian Forest Health Initiative, the Northern Research Station of the U.S. Forest Service in the U.S. Department of Agriculture, the Hea lthy Forest Partnership Early Intervention Strategy financed by the Federal Government of Canada in partnership with participating Provinces and forest industry, and the Department of Forest and Wildlife Ecology in the College of Agriculture and Life Sciences at UW–Madison.

Supplemental materials

Supplemental materials associated with this article can be found, in the online version, at doi:10.1016/j.agrformet.2022.108815.

References

Berryman, A.A., 1982. Biological control, thresholds, and pest outbreaks. Environ. Entomol. 11, 544–549. https://doi.org/10.1093/ee/11.3.544.

Berryman, A.A., 1996. What causes population cycles of forest Lepidoptera? Trends Ecol. Evol. 11, 28–32. https://doi.org/10.1016/0169-5347(96)81066-4 (Amst.).

Bonte, D., Dahirel, M., 2017. Dispersal: a central and independent trait in life history. Oikos 126, 472–479. https://doi.org/10.1111/oik.03801.

Bouchard, M., Auger, I., 2014. Influence of environmental factors and spatio-temporal covariates during the initial development of a spruce budworm outbreak. Landsc. Ecol. 29, 111–126. https://doi.org/10.1007/s10980-013-9966-x.

Bouchard, M., Kneeshaw, D., Messier, C., 2007. Forest dynamics following spruce budworm outbreaks in the northern and southern mixedwoods of central Quebec. Can. J. For. Res. 37, 763–772. https://doi.org/10.1139/X06-278.

Bouchard, M., Martel, V., Régnière, J., Therrien, P., Correia, D.L.P., 2018a. Do natural enemies explain fluctuations in low-density spruce budworm populations? Ecology 99, 2047–2057. https://doi.org/10.1002/ecy.2417.

Bouchard, M., Régnière, J., Therrien, P., 2018b. Bottom-up factors contribute to large-scale synchrony in spruce budworm populations. Can. J. For. Res. 48, 277–284. https://doi.org/10.1139/cjfr-2017-0051.

Boulanger, Y., Arseneault, D., 2004. Spruce budworm outbreaks in eastern Quebec over the last 450 years. Can. J. For. Res. 34, 1035–1043. https://doi.org/10.1139/x03-269.

Boulanger, Y., Arseneault, D., Morin, H., Jardon, Y., Bertrand, P., Dagneau, C., 2012. Dendrochronological reconstruction of spruce budworm (*Choristoneura fumiferana*) outbreaks in southern Quebec for the last 400 years. Can. J. For. Res. 42, 1264–1276. https://doi.org/10.1139/x2012-069.

Boulanger, Y., Fabry, F., Kilambi, A., Pureswaran, D.S., Sturtevant, B.R., Saint-Amant, R., 2017. The use of weather surveillance radar and high-resolution three dimensional weather data to monitor a spruce budworm mass exodus flight. Agric. For. Meteorol. 234–235, 127–135. https://doi.org/10.1016/j.agrformet.2016.12.018.

Candau, J.-N., Fleming, R.A., Hopkin, A., 1998. Spatiotemporal patterns of large-scale defoliation caused by the spruce budworm in Ontario since 1941. Can. J. For. Res. 28, 1733–1743. https://doi.org/10.1139/x98-164.

Chapman, J.W., Nilsson, C., Lim, K.S., Bäckman, J., Reynolds, D.R., Alerstam, T., 2016. Adaptive strategies in nocturnally migrating insects and songbirds: contrasting responses to wind. J. Anim. Ecol. 85, 115–124. https://doi.org/10.1111/1365-2656.12420.

Chapman, J.W., Reynolds, D.R., Wilson, K., 2015. Long-range seasonal migration in insects: mechanisms, evolutionary drivers and ecological consequences. Ecol. Lett. 18, 287–302. https://doi.org/10.1111/ele.12407.

Contarini, M., Onufrieva, K.S., Thorpe, K.W., Raffa, K.F., Tobin, P.C., 2009. Mate-finding failure as an important cause of Allee effects along the leading edge of an invading insect population. Entomol. Exp. Appl. 133, 307–314. https://doi.org/10.1111/j.1570-7458.2009.00930.x.

Delisle, J., Hardy, M., 1997. Male larval nutrition influences the reproductive success of both sexes of the spruce budworm, *Choristoneura fumiferana* (Lepidoptera: tortricidae). Funct. Ecol. 11, 451–463. https://doi.org/10.1046/j.1365-2435.1997.00114.x.

Dickison, R.B.B., Haggis, M.J., Rainey, R.C., 1983. Spruce budworm moth flight and storms: case study of a cold front system. J. Clim. Appl. Meteorol. 22, 278–286. https://doi.org/10.1175/1520-0450(1983)022<0278:SBMFAS>2.0.CO;2.

Dickison, R.B.B., Haggis, M.J., Rainey, R.C., Burns, L.M.D., 1986. Spruce budworm moth flight and storms: further studies using aircraft and radar. J. Clim. Appl. Meteorol. 25, 1600–1608. https://doi.org/10.1175/1520-0450(1986)025<1600:SBMFAS>2.0.CO;2.

Dickison, R.B.B., Mason, P.J., Browning, K.A., Lunnon, R.W., Pedgley, D.E., Riley, J.R., Joyce, R.J.V., Rainey, R.C., Browning, K.A., Cheke, R.A., Haggis, M.J., 1990. Detection of mesoscale synoptic features associated with dispersal of spruce budworm moths in eastern Canada. Philos. Trans. R. Soc. Lond. B Biol. Sci. 328, 607–617. https://doi.org/10.1098/rstb.1990.0131.

Drake, V.A., 1984. The vertical distribution of macro-insects migrating in the nocturnal boundary layer: a radar study. Bound. Layer Meteorol. 28, 353–374. https://doi.org/10.1007/BF00121314.

Drake, V.A., 1985. Radar observations of moths migrating in a nocturnal low-level jet. Ecol. Entomol. 10, 259–265. https://doi.org/10.1111/j.1365-2311.1985.tb00722.x.

Frago, E., Bauce, É., 2014. Life-history consequences of chronic nutritional stress in an outbreaking insect defoliator. PLoS One 9, e88039. https://doi.org/10.1371/journal.pone.0088039.

Gauthreaux, S., Diehl, R., 2020. Discrimination of biological scatterers in polarimetric weather radar data: opportunities and challenges. Remote Sens. 12, 545. https://doi.org/10.3390/rs12030545 (Basel).

Greenbank, D.O., 1957. The role of climate and dispersal in the initiation of outbreaks of the spruce budworm in New Brunswick: II. The role of dispersal. Can. J. Zool. 35, 385–403. https://doi.org/10.1139/z57-029.

Greenbank, D.O., Schaefer, G.W., Rainey, R.C., 1980. Spruce budworm (Lepidoptera: tortricidae) moth flight and dispersal: new understanding from canopy observations, radar, and aircraft. Mem. Entomol. Soc. Can. 112, 1–49. https://doi.org/10.4039/entm112110fv.

Grimm, V., Berger, U., Bastiansen, F., Eliassen, S., Ginot, V., Giske, J., Goss-Custard, J., Grand, T., Heinz, S.K., Huse, G., Huth, A., 2006. A standard protocol for describing individual-based and agent-based models. Ecol. Model. 198, 115–126. https://doi.org/10.1016/j.ecolmodel.2006.04.023.

Grimm, V., Berger, U., DeAngelis, D.L., Polhill, J.G., Giske, J., Railsback, S.F., 2010. The ODD protocol: a review and first update. Ecol. Model. 221, 2760–2768. https://doi.org/10.1016/j.ecolmodel.2010.08.019.

Hennigar, C.R., MacLean, D.A., Quiring, D.T., Kershaw Jr., J.A., 2008. Differences in spruce budworm defoliation among balsam fir and white, red, and black spruce. Forest Science 54, 158–166. https://doi.org/10.1093/forestscience/54.2.158.

Isard, S.A., Gage, S.H., Comtois, P., Russo, J.M., 2005. Principles of the atmospheric pathway for invasive species applied to soybean rust. Bioscience 55, 851–861. https://doi.org/10.1641/0006-3568(2005)055[0851:POTAPF]2.0.CO;2.

Johns, R.C., Bowden, J.J., Carleton, D.R., Cooke, B.J., Edwards, S., Emilson, E.J.S., James, P.M.A., Kneeshaw, D., MacLean, D.A., Martel, V., Moise, E.R.D., Mott, G.D., Norfolk, C.J., Owens, E., Pureswaran, D.S., Quiring, D.T., Régnière, J., Richard, B., Stastny, M., 2019. A conceptual framework for the spruce budworm early intervention strategy: can outbreaks be stopped? Forests 10, 910. https://doi.org/10.3390/f10100910.

Koralewski, T.E., Wang, H.H., Grant, W.E., Brewer, M.J., Elliott, N.C., Westbrook, J.K., 2021. Modeling the dispersal of wind-borne pests: sensitivity of infestation forecasts to uncertainty in parameterization of long-distance airborne dispersal. Agric. For. Meteorol. 301–302, 108357 https://doi.org/10.1016/j.agrformet.2021.108357.

Lakovic, M., Poethke, H.J., Hovestadt, T., 2015. Dispersal timing: emigration of insects living in patchy environments. PLoS One 10, e0128672. https://doi.org/10.1371/journal.pone.0128672.

Liebhold, A., Koenig, W.D., Bjørnstad, O.N., 2004. Spatial synchrony in population dynamics. Annu. Rev. Ecol. Evol. Syst. 35, 467–490. https://doi.org/10.1146/annurev.ecolsys.34.011802.132516.

Luo, Y., Berbery, E.H., Mitchell, K.E., Betts, A.K., 2007. Relationships between land surface and near-surface atmospheric variables in the NCEP North American regional reanalysis. J. Hydrometeorol. 8, 1184–1203. https://doi.org/10.1175/2007JHM844.1.

MacLean, D.A., 1980. Vulnerability of fir-spruce stands during uncontrolled spruce budworm outbreaks: a review and discussion. For. Chron. 56, 213–221. https://doi.org/10.5558/tfc56213-5.

MacLean, D.A., 2019. Protection strategy against spruce budworm. Forests 10, 1137. https://doi.org/10.3390/f10121137.

MacLean, D.A., Amirault, P., Amos-Binks, L., Carleton, D., Hennigar, C., Johns, R., Régnière, J., 2019. Positive results of an early intervention strategy to suppress a spruce budworm outbreak after five years of trials. Forests 10, 448. https://doi.org/10.3390/f10050448.

MacLean, D.A., MacKinnon, W.E., 1996. Accuracy of aerial sketch-mapping estimates of spruce budworm defoliation in New Brunswick. Can. J. For. Res. 26, 2099–2108. https://doi.org/10.1139/x26-238.
Mesinger, F., DiMego, G., Kalnay, E., Mitchell, K., Shafran, P.C., Ebisuzaki, W., Jović, D., Woollen, J., Rogers, E., Berbery, E.H., Ek, M.B., Fan, Y., Grumbine, R., Higgins, W., Li, H., Lin, Y., Manikin, G., Parrish, D., Shi, W., 2006. North American regional reanalysis. Bull. Am. Meteorol. Soc. 87, 343–360. https://doi.org/10.1175/BAMS-87-3-343.
Miller, C.A., Greenbank, D.O., Kettela, E.G., 1978. Estimated egg deposition by invading spruce budworm moths (Lepidoptera: tortricidae). Can. Entomol. 110, 609–615. https://doi.org/10.4039/Ent110609-6.
Nealis, V.G., Régnière, J., 2004. Fecundity and recruitment of eggs during outbreaks of the spruce budworm. Can. Entomol. 136, 591–604. https://doi.org/10.4039/n03-089.
Nenzén, H.K., Peres-Neto, P., Gravel, D., 2018. More than Moran: coupling statistical and simulation models to understand how defoliation spread and weather variation drive insect outbreak dynamics. Can. J. For. Res. 48, 255–264. https://doi.org/10.1139/cjfr-2016-0396.
Parry, D., Spence, J., Volney, W., 1997. Responses of natural enemies to experimentally increased populations of the forest tent caterpillar, Malacosoma disstria. Ecol. Entomol. 22, 97–108. https://doi.org/10.1046/j.1365-2311.1997.00022.x.
Pedgley, D.E., Scorer, R.S., Purdom, J.F.W., Simpson, J.E., Wickham, P.G., Dickison, R.B. B., Morris, R.M., Drake, V.A., 1990. Concentration of flying insects by the wind. Philos. Trans. R. Soc. Lond. B Biol. Sci. 328, 631–653. https://doi.org/10.1098/rstb.1990.0133.
Peltonen, M., Liebhold, A.M., Bjørnstad, O.N., Williams, D.W., 2002. Spatial synchrony in forest insect outbreaks: roles of regional stochasticity and dispersal. Ecology 83, 3120–3129. https://doi.org/10.1890/0012-9658(2002)083[3120:SSIFIO]2.0.CO;2.
Powers, J.G., and 24 coauthors, 2017. The Weather Research and Forecasting model: overview, system efforts, and future directions. Bull. Am. Meteorol. Soc. 98, 1717–1737. https://doi.org/10.1175/BAMS-D-15-00308.1.
Quezada-García, R., Bauce, É., 2013. Heritability of life-history traits in the spruce budworm. Entomol. Sci. 17, 111–117. https://doi.org/10.1111/ens.12031.
Régnière, J., 1983. An oviposition model for the spruce budworm, *Choristoneura fumiferana* (Lepidoptera: tortricidae). Can. Entomol. 115, 1371–1382. https://doi.org/10.4039/Ent1151371-10.
Régnière, J., 1996. Generalized approach to landscape-wide seasonal forecasting with temperature-driven simulation models. Environ. Entomol. 25, 869–881. https://doi.org/10.1093/ee/25.5.869.
Régnière, J., Bolstad, P., 1994. Statistical simulation of daily air temperature patterns in eastern North America to forecast seasonal events in insect pest management. Environ. Entomol. 23, 1368–1380. https://doi.org/10.1093/ee/23.6.1368.
Régnière, J., Cooke, B.J., Béchard, A., Dupont, A., Therrien, P., 2019a. Dynamics and management of rising outbreak spruce budworm populations. Forests 10, 748. https://doi.org/10.3390/f10090748.
Régnière, J., Delisle, J., Dupont, A., Trudel, R., 2019b. The impact of moth migration on apparent fecundity overwhelms mating disruption as a method to manage spruce budworm populations. Forests 10, 775. https://doi.org/10.3390/f10090775.
Régnière, J., Delisle, J., Pureswaran, D.S., Trudel, R., 2013. Mate-finding Allee effect in spruce budworm population dynamics. Entomol. Exp. Appl. 146, 112–122. https://doi.org/10.1111/eea.12019.
Régnière, J., Delisle, J., Sturtevant, B.R., Garcia, M., Saint-Amant, R., 2019c. Modeling migratory flight in the spruce budworm: temperature constraints. Forests 10, 802. https://doi.org/10.3390/f10090802.
Régnière, J., Garcia, M., Saint-Amant, R., 2019d. Modeling migratory flight in the spruce budworm: circadian rhythm. Forests 10, 877. https://doi.org/10.3390/f10100877.
Régnière, J., Lavigne, D., Dickison, R., Staples, A., 1995. Performance Analysis of BioSIM, a Seasonal Pest Management Planning tool, in New Brunswick in 1992 and 1993. Natural Resources Canada, Canadian Forest Service, Laurentian Forestry Centre, Sainte-Foy, QC. Information Report LAU-X-115.
Régnière, J., Lysyk, T.J., 1995. Population dynamics of the spruce budworm, *Choristoneura fumiferana*. In: Armstrong, J.A., Ives, W.G.H. (Eds.), Forest Insect Pests in Canada. Natural Resources Canada, Canadian Forest Service, Ottawa, ON, Canada, pp. 95–105.
Régnière, J., Nealis, V.G., 2007. Ecological mechanisms of population change during outbreaks of the spruce budworm. Ecol. Entomol. 32, 461–477. https://doi.org/10.1111/j.1365-2311.2007.00888.x.
Régnière, J., Nealis, V.G., 2019. Density dependence of egg recruitment and moth dispersal in spruce budworms. Forests 10, 706. https://doi.org/10.3390/f10080706.
Régnière, J., St-Amant, R., 2007. Stochastic simulation of daily air temperature and precipitation from monthly normals in North America north of Mexico. Int. J. Biometeorol. 51, 415–430. https://doi.org/10.1007/s00484-006-0078-z.
Régnière, J., Saint-Amant, R., Duval, P., 2012. Predicting insect distributions under climate change based on physiological responses: spruce budworm as an example. Biol. Invasions 14, 1–16. https://doi.org/10.1007/s10530-010-9918-1.
Régnière, J., St-Amant, R., Béchard, A., 2014. BioSIM 10 User's Manual. Natural Resources Canada, Canadian Forest Service, Laurentian Forestry Centre, Quebec, QC Canada. Information Report LAU-X-137E. https://cfs.nrcan.gc.ca/publications/download-pdf/34818.
Reynolds, D.R., Chapman, J.W., Edwards, A.S., Smith, A.D., Wood, C.R., Barlow, J.F., Woiwod, I.P., 2005. Radar studies of the vertical distribution of insects migrating over southern Britain: the influence of temperature inversions on nocturnal layer concentrations. Bull. Entomol. Res. 95, 259–274. https://doi.org/10.1079/BER2005358.
Reynolds, D.R., Smith, A.D., Chapman, J.W., 2008. A radar study of emigratory flight and layer formation by insects at dawn over southern Britain. Bull. Entomol. Res. 98, 35–52. https://doi.org/10.1017/S0007485307005470.
Rhainds, M., 2010. Female mating failures in insects. Entomol. Exp. Appl. 136, 211–226. https://doi.org/10.1111/j.1570-7458.2010.01032.x.
Rhainds, M., 2020. Variation in wing load of female spruce budworms (Lepidoptera: tortricidae) during the course of an outbreak: evidence for phenotypic response to habitat deterioration in collapsing populations. Environ. Entomol. 49, 238–245. https://doi.org/10.1093/ee/nvz144.
Rhainds, M., Kettela, E.G., 2013. Oviposition threshold for flight in an inter-reproductive migrant moth. J. Insect. Behav. 26, 850–859. https://doi.org/10.1007/s10905-013-9400-x.
Riley, J.R., Reynolds, D.R., Farmery, M.J., 1983. Observations of the flight behaviour of the army worm moth, *Spodoptera exempta*, at an emergence site using radar and infra-red optical techniques. Ecol. Entomol. 8, 395–418. https://doi.org/10.1111/j.1365-2311.1983.tb00519.x.
Royama, T., 1984. Population dynamics of the spruce budworm *Choristoneura fumiferana*. Ecol. Monogr. 54, 429–462. https://doi.org/10.2307/1942595.
Royama, T., 2005. Moran effect on nonlinear population processes. Ecol. Monogr. 75, 277–293. https://doi.org/10.1890/04-0770.
Sanders, C.J., Lucuik, G.S., 1975. Effects of photoperiod and size on flight activity and oviposition in the eastern spruce budworm (Lepidoptera: tortricidae). Can. Entomol. 107, 1289–1299. https://doi.org/10.4039/Ent1071289-12.
Sanders, C.J., Wallace, D.R., Lucuik, G.S., 1978. Flight activity of female eastern spruce budworm (Lepidoptera: tortricidae) at constant temperatures in the laboratory. Can. Entomol. 110, 627–632. https://doi.org/10.4039/Ent110627-6.
Satterfield, D.A., Sillett, T.S., Chapman, J.W., Altizer, S., Marra, P.P., 2020. Seasonal insect migrations: massive, influential, and overlooked. Front. Ecol. Environ. 18, 335–344. https://doi.org/10.1002/fee.2217.
Schaefer, G.W., 1976. Radar observations of insect flight. Symp. R. Entomol. Soc. Lond. 7, 157–197.
Scott, R.W., Achtemeier, G.L., 1987. Estimating pathways of migrating insects carried in atmospheric winds. Environ. Entomol. 16, 1244–1254. https://doi.org/10.1093/ee/16.6.1244.
Showers, W.B., 1997. Migratory ecology of the black cutworm. Annu. Rev. Entomol. 42, 393–425. https://doi.org/10.1146/annurev.ento.42.1.393.
Showers, W.B., Whitford, F., Smelser, R.B., Keaster, A.J., Robinson, J.F., Lopez, J.D., Taylor, S.E., 1989. Direct evidence for meteorologically driven long-range dispersal of an economically important moth. Ecology 70, 987–992. https://doi.org/10.2307/1941366.
Skamarock, W.C., Klemp, J.B., 2008. A time-split nonhydrostatic atmospheric model for weather research and forecasting applications. J. Comput. Phys. 227, 3465–3485. https://doi.org/10.1016/j.jcp.2007.01.037.
Skamarock, W.C., Klemp, J.B., Dudhia, J., Gill, D.O., Barker, D.M., Duda, M.G., Huang, X. Y., Wang, W., Powers, J.G., 2008. A Description of the Advanced Research WRF Version 3. NCAR Tech. https://doi.org/10.5065/D68S4MVH. Note NCAR/TN-475+STR, 113 pp.
Smith, M.J., Sherratt, J.A., Lambin, X., 2008. The effects of density-dependent dispersal on the spatiotemporal dynamics of cyclic populations. J. Theor. Biol. 254, 264–274. https://doi.org/10.1016/j.jtbi.2008.05.034.
Stein, A.F., Draxler, R.R., Rolph, G.D., Stunder, B.J.B., Cohen, M.D., Ngan, F., 2015. NOAA's HYSPLIT atmospheric transport and dispersion modeling system. Bull. Am. Meteorol. Soc. 96, 2059–2077. https://doi.org/10.1175/BAMS-D-14-00110.1.
Stepanian, P.M., Horton, K.G., Melnikov, V.M., Zrnić, D.S., Gauthreaux, S.A., 2016. Dual-polarization radar products for biological applications. Ecosphere 7, e01539. https://doi.org/10.1002/ecs2.1539.
Stephens, P.A., Sutherland, W.J., Freckleton, R.P., 1999. What is the Allee effect? Oikos 87, 185–190. https://doi.org/10.2307/3547011.
Stohl, A., Forster, C., Frank, A., Seibert, P., Wotawa, G., 2005. Technical note: the Lagrangian particle dispersion model FLEXPART version 6.2. Atmos. Chem. Phys. 5, 2461–2474. https://doi.org/10.5194/acp-5-2461-2005.
Sturtevant, B.R., Achtemeier, G.L., Charney, J.J., Anderson, D.P., Cooke, B.J., Townsend, P.A., 2013. : long-distance dispersal of spruce budworm (*Choristoneura fumiferana* Clemens) in Minnesota (USA) and Ontario (Canada) via the atmospheric pathway. Agric. For. Meteorol. 168, 186–200. https://doi.org/10.1016/j.agrformet.2012.09.008.
Taylor, C.M., Hastings, A., 2005. Allee effects in biological invasions. Ecol. Lett. 8, 895–908. https://doi.org/10.1111/j.1461-0248.2005.00787.x.
Taylor, S.L., MacLean, D.A., 2008. Validation of spruce budworm outbreak history developed from aerial sketch mapping of defoliation in New Brunswick. North. J. Appl. For. 25, 139–145. https://doi.org/10.1093/njaf/25.3.139.
Tobin, P.C., Robinet, C., Johnson, D.M., Whitmire, S.L., Bjørnstad, O.N., Liebhold, A.M., 2009. The role of Allee effects in gypsy moth, *Lymantria dispar* (L.), invasions. Popul. Ecol. 51, 373–384. https://doi.org/10.1007/s10144-009-0144-6.
Van Hezewijk, B., Wertman, D., Stewart, D., Béliveau, C., Cusson, M., 2018. Environmental and genetic influences on the dispersal propensity of spruce budworm (*Choristoneura fumiferana*). Agric. For. Entomol. 20, 433–441. https://doi.org/10.1111/afe.12275.
Wang, H.H., Grant, W.E., Elliott, N.C., Brewer, M.J., Koralewski, T.E., Westbrook, J.K., Alves, T.M., Sword, G.A., 2019. : integrated modelling of the life cycle and aeroecology of wind-borne pests in temporally-variable spatially-heterogeneous environment. Ecol. Model. 399, 23–38. https://doi.org/10.1016/j.ecolmodel.2019.02.014.
Wang, H.H., Grant, W.E., Koralewski, T.E., Brewer, M.J., Elliott, N.C., 2021. Simulating migration of wind-borne pests: "Deconstructing" representation of the emigration

process. Ecol. Model. 460, 109742 https://doi.org/10.1016/j.ecolmodel.2021.109742.
Westbrook, J.K., Eyster, R.S., 2017. : doppler weather radar detects emigratory flights of noctuids during a major pest outbreak. Remote Sens. Appl. Soc. Environ. 8, 64–70. https://doi.org/10.1016/j.rsase.2017.07.009.
Westbrook, J.K., Eyster, R.S., Wolf, W.W., 2014. WSR-88D doppler radar detection of corn earworm moth migration. Int. J. Biometeorol. 58, 931–940. https://doi.org/10.1007/s00484-013-0676-5.
Westbrook, J., Fleischer, S., Jairam, S., Meagher, R., Nagoshi, R., 2019. Multigenerational migration of fall armyworm, a pest insect. Ecosphere 10, e02919. https://doi.org/10.1002/ecs2.2919.
Westbrook, J.K., Isard, S.A., 1999. Atmospheric scales of biotic dispersal. Agric. For. Meteorol. 97, 263–274. https://doi.org/10.1016/S0168-1923(99)00071-4.
Westbrook, J.K., Nagoshi, R.N., Meagher, R.L., Fleischer, S.J., Jairam, S., 2016. Modeling seasonal migration of fall armyworm moths. Int. J. Biometeorol. 60, 255–267. https://doi.org/10.1007/s00484-015-1022-x.
Williams, D.W., Liebhold, A.M., 2000. : spatial synchrony of spruce budworm outbreaks in eastern North America. Ecology 81, 2753–2766. https://doi.org/10.1890/0012-9658(2000)081[2753:SSOSBO]2.0.CO;2.
Wood, C.R., Chapman, J.W., Reynolds, D.R., Barlow, J.F., Smith, A.D., Woiwod, I.P., 2006. The influence of the atmospheric boundary layer on nocturnal layers of noctuids and other moths migrating over southern Britain. Int. J. Biometeorol. 50, 193. https://doi.org/10.1007/s00484-005-0014-7.
Wood, C.R., Reynolds, D.R., Wells, P.M., Barlow, J.F., Woiwod, I.P., Chapman, J.W., 2009. Flight periodicity and the vertical distribution of high-altitude moth migration over southern Britain. Bull. Entomol. Res. 99, 525–535. https://doi.org/10.1017/S0007485308006548.
Wood, C.R., Clark, S.J., Barlow, J.F., Chapman, J.W., 2010. Layers of nocturnal insect migrants at high-altitude: the influence of atmospheric conditions on their formation. Agric. For. Entomol. 12, 113–121. https://doi.org/10.1111/j.1461-9563.2009.00459.x.
Wu, Q.L., Hu, G., Westbrook, J.K., Sword, G.A., Zhai, B.P., 2018. An advanced numerical trajectory model tracks a corn earworm moth migration event in Texas, USA. Insects 9, 115. https://doi.org/10.3390/insects9030115.
Zhang, Z., Zhang, Y., Wang, J., Liu, J., Tang, Q., Li, X., Cheng, D., Zhu, X., 2018. Analysis on the migration of first-generation *Mythimna separata* (Walker) in China in 2013. J. Integr. Agric. 17, 1527–1537. https://doi.org/10.1016/S2095-3119(17)61885-9.
Zrnic, D.S., Ryzhkov, A.V., 1998. Observations of insects and birds with a polarimetric radar. IEEE Trans. Geosci. Remote Sens. 36, 661–668. https://doi.org/10.1109/36.662746.